NATIONAL ENERGY TECHNOLOGY LABORATORY

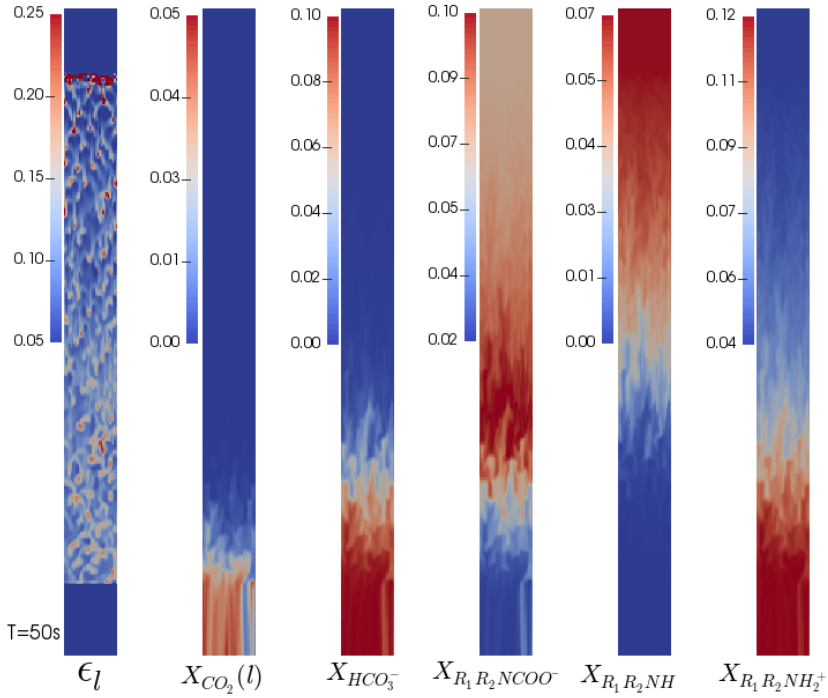

Device Scale Modeling of Solvent Absorption using MFIX-TFM

October 2016

U.S. DEPARTMENT OF ENERGY | NATIONAL ENERGY TECHNOLOGY LABORATORY

Office of Fossil Energy

NETL-PUB-20902

Disclaimer

Cover Illustration: Removal of CO_2 from a gas stream through absorption into an aqueous monoethanolamine (MEA) liquid solvent. Visualization shows the instantaneous liquid fraction (ϵ_l) and liquid species mass fractions (X) in a counter-flow gas-liquid absorption column, as predicted by an MFIX-TFM simulation. Additional simulation details are described in Section 6 of this report.

Suggested Citation: Carney, J. E. and Finn, J. R.; *Device Scale Modeling of Solvent Absorption using MFIX-TFM*; NETL-PUB-20902; NETL Technical Report Series; U.S. Department of Energy, National Energy Technology Laboratory: Albany, OR, 2016; p 48.

An electronic version of this report can be found at:

http://www.netl.doe.gov/research/on-site-research/publications/featured-technical-reports

http://www.osti.gov/bridge

CFD Modeling for Solvent Absorption in MFIX

Janine E. Carney[1], Justin R. Finn[1,2]

[1] U.S. Department of Energy, National Energy Technology Laboratory, 1450 Queen Avenue SW, Albany, OR 97321

[2] Oakridge Institute for Science and Education, MC-100-44, P.O. Box 117, Oak Ridge, TN, 37831

NETL-TRS-20902-2016

October 2016

NETL Contacts:

Janine E. Carney, Principal Investigator

David Miller, Technical Portfolio Lead

Cynthia Powell, Executive Director, Research & Innovation Center

This page intentionally left blank.

Table of Contents

List of Figures

List of Tables

Acronyms, Abbreviations, and Symbols

Term	Description
Abbreviations	
MEA	Monoethanolamine, the chemical solvent considered in this study
MFIX	Multiphase Flow with Interphase eXchanges, a CFD software
TFM	Two-fluid model, a framework used for multiphase flow simulation.
Symbols	
A	Heat transfer area
a	Surface area per unit volume of bed (interfacial area when no subscript)
A, B, C	Constants
C_p	Specific heat
$\mathcal{D}$	Diffusion coefficient
$\mathbf{D}$	Rate of strain tensor
D_p	Nominal size of packing material
d_p	Surface-to-volume effective particle diameter ($6V_p/S_p = 6(1-\epsilon)/a_t$)
E, E_i, E_1	Enhancement factor(s)
F	Interphase momentum exchange coefficient(s)
$\mathbf{F_D}$	Mechanical dispersion force
$\mathbf{g}$	Gravitational acceleration
G	Superficial mass velocity of the gas
H	Henry's constant
Ha	Hatta number
h	Specific enthalpy
$\mathbf{I}$	Identity tensor
J	Leverett's J function for saturation
k	Reaction rate constant
K	Equilibrium constant
k_g	Gas-side mass transfer coefficient
k_l	Liquid-side mass transfer coefficient
k_l^0	Liquid-side physical mass transfer coefficient (without enhancement)
L	Superficial mass velocity of the liquid; Characteristic length
$\dot{m}$	Mass flow rate
N	Number of species
Nu	Nusselt number
p	Partial pressure
P	Pressure
Pr	Prandtl number
R	Rate of formation
Re	Reynolds number
S	Heat transfer source term
S_p	Particle surface area
s	Saturation ($s_i = \varepsilon_i/\epsilon$)
S_f	Spread factor used for mechanical dispersion
T	Thermal temperature
$\mathbf{u}$	Velocity

Term	Description
$\mathbf{u}_D$	Drift velocity
V_p	Particle Volume
X	Mass fraction
Greek Symbols	
ϵ	Porosity
ε	Volume fraction
κ	Permeability
λ	Thermal conductivity
ρ	Density
σ	Surface tension
$\boldsymbol{\tau}$	Shear stress
μ	Molecular viscosity
γ	Heat transfer coefficient
Subscripts / Superscripts	
c	Capillary pressure; critical surface tension
fwd	Forward
g	Gas phase
i	Phase index
$interface$	Property of the gas-liquid interface
l	Liquid phase
n	Species index
rvs	Reverse
s	Solid phase
t	Total
w	Wetted

Acknowledgments

This work was completed as part of National Energy Technology Laboratory (NETL) research for the U.S. Department of Energy's (DOE) Complementary Research Program under Section 999 of the Energy Policy Act of 2005. The authors wish to acknowledge Xin Sun, Pacific Northwest National Laboratory (PNNL), and David Miller, NETL, for programmatic guidance, direction, and support.

The authors would also like to thank Sankaran Sundaresan (Princeton University) for fundamental insight and technical discussion on modeling gas-liquid multiphase flow.

ABSTRACT

Recent climate change is largely attributed to greenhouse gases (e.g., carbon dioxide, methane) and fossil fuels account for a large majority of global CO_2 emissions. That said, fossil fuels will continue to play a significant role in the generation of power for the foreseeable future. The extent to which CO_2 is emitted needs to be reduced, however, carbon capture and sequestration are also necessary actions to tackle climate change. Different approaches exist for CO_2 capture including both post-combustion and pre-combustion technologies, oxy-fuel combustion and/or chemical looping combustion. The focus of this effort is on post-combustion solvent-absorption technology.

To apply CO_2 technologies at commercial scale, the availability and maturity and the potential for scalability of that technology need to be considered. Solvent absorption is a proven technology but not at the scale needed by typical power plant. The scale up and down and design of laboratory and commercial packed bed reactors depends heavily on the specific knowledge of two-phase pressure drop, liquid holdup, the wetting efficiency and mass transfer efficiency as a function of operating conditions. Simple scaling rules often fail to provide proper design. Conventional reactor design modeling approaches will generally characterize complex non-ideal flow and mixing patterns using simplified and/or mechanistic flow assumptions. While there are varying levels of complexity used within these approaches, none of these models resolve the local velocity fields. Consequently, they are unable to account for important design factors such as flow maldistribution and channeling from a fundamental perspective.

Ideally design would be aided by development of predictive models based on truer representation of the physical and chemical processes that occur at different scales. Computational fluid dynamic (CFD) models are based on multidimensional flow equations with first principle foundations. CFD models can include a more accurate physical description of flow processes and be modified to include more complex behavior. Wetting performance and spatial liquid distribution inside the absorber are recognized as weak areas of knowledge requiring further investigation. CFD tools offer a possible method to investigating such topics and gaining a better understanding of their influence on reactor performance.

This report focuses first on describing a hydrodynamic model for countercurrent gas-liquid flow through a packed column and then on the chemistry, heat and mass transfer specific to CO_2 absorption using monoethanolamine (MEA). The indicated model is implemented in MFIX, a CFD open source software package. The user defined functions needed to build this model are described in detail along with the keywords for the corresponding input file. A test case is outlined along with a few results. The example serves to briefly illustrate the developed CFD tool and its potential capability to investigate solvent absorption.

1. INTRODUCTION

One method to remove CO_2 from a gas stream is through absorption into a liquid solvent. The absorption can be classified as physical or chemical absorption with chemical solvents preferred due to higher absorption efficiency. Solvent absorption is usually carried out in a countercurrent tower where the gas ascends and the liquid descends. The purpose is to preferentially dissolve one or more of the constituents of the gas, such as carbon dioxide (CO_2), into the liquid. The dissolved constituents are termed solutes, while the dissolving liquid is termed the solvent. The tower is filled with packing that provides the surface area for gas-liquid contact. Surface area is important because very little reaction will occur without adequate mixing of the gas and liquid. For example, if gas is simply bubbled through a tank of liquid some mixing will occur, but reaction only occurs where the gas and liquid meet resulting in a low efficiency.

One of the main challenges in developing a CFD model for solvent absorption is that it is a multi-scale problem. The column size is characterized by length scales of several meters while the characteristic dimensions of the packing are much smaller. For example, random packings, such as Raschig or Pall Rings, typically have dimensions ranging from 25-80mm (Mackowiak, 2010). The length scale of a typical layer of corrugated structured packing is on the order of 20 centimeters (Raynal, Ben Rayana, & Royon-Lebeaud, 2009). The corrugation height varies with the specific area of the packing from a few millimeters to several centimeters (Raynal, Boyer, & Ballaguet, 2004). Finally the dimension of liquid film thickness is on the order of tenths of millimeters for structured packing (Raynal et al., 2009). These scales cannot be resolved simultaneously within a single computational model; it is computationally infeasible to run computations at large scales while taking into account the gas-liquid interaction and the real geometry of the packing. The present effort focuses on the development of a basic CFD model for device scale simulations.

The fluid dynamics of the liquid film is important in solvent absorption because efficiency of CO_2 absorption is closely related to structure of liquid films within packing [8]. The Volume of Fluid (VOF) model is an appropriate numerical method for simulating of two phase flows where the interface between the gas-liquid phases important. Unfortunately, the VOF method requires the detailed geometry of the packing element cells to be resolved, so these types of simulations are confined to small volume due to computational constraints. Thus, for modeling a large-scale device an Eulerian-Eulerian technique is more appropriate, and may be the most computationally feasible approach for some time. This report focuses on development of such a model and its integration in the MFIX-TFM (Two Fluid Model) framework. MFIX (Multiphase Flow with Interphase eXchanges) is an open-source computer code developed at DOE NETL that is designed to describe the hydrodynamics, heat transfer and chemical reactions in multiphase systems (Syamlal, Rogers, & O'Brien, 1993).

2. METHOD/THEORY: CONSERVATION EQUATIONS

In the Eulerian-Eulerian approach the different phases are mathematically treated as interpenetrating continua. The volume fractions of each phase are assumed to be a continuous function of space and time and their sum is equal to unity. The conservation equations are typically derived based on the application of averaging (e.g., volume, time, or ensemble) to the microscopic description of the system. The resulting set of equations have similar structure, however, the process leads to a number of unknown terms that require constitutive relations for closure. Shown below are the continuity and momentum equations used in a reactive flow simulation for gas-liquid systems (e.g. (Dudukovic, Larachi, & Mills, 2002; Gunjal, Kashid, Ranade, & Chaudhari, 2005)).

$$\frac{\partial}{\partial t}(\varepsilon_i \rho_i) + \nabla \cdot (\varepsilon_i \rho_i \mathbf{u}_i) = \sum_{n=1}^{N_i} R_{in} \tag{1}$$

$$\frac{\partial}{\partial t}(\varepsilon_i \rho_i \mathbf{u}_i) + \nabla \cdot (\varepsilon_i \rho_i \mathbf{u}_i \mathbf{u_i}) = -\varepsilon_i \nabla P_i + \nabla \cdot (\varepsilon_i \boldsymbol{\tau}_i) + \varepsilon_i \rho_i \mathbf{g} - F_{ij}(\mathbf{u}_i - \mathbf{u}_j) - F_{si}\mathbf{u}_i + \mathbf{F}_{Di} \tag{2}$$

Here ε_i represents the volume fraction of the i^{th} phase, ρ_i is the density of the i^{th} phase, $\mathbf{u_i}$ is the cell velocity of the i^{th} phase, N_i is the number of chemical species comprising the i^{th} phase and R_{in} represents the rate of formation of the n^{th} species in the i^{th} phase. The term on the right hand side represents the formation or consumption of mass attributed to interphase mass transfer from chemical reactions or physical processes. In the momentum balance, P_i is the i^{th} phase pressure, $\boldsymbol{\tau}_i$ is the shear stress, $\mathbf{g}$ is gravitational acceleration, F_{ij} and F_{si} are the interphase momentum exchange terms and $\mathbf{F}_{Di}$ is a mechanical dispersion term. The respective terms on the right-hand side represent the pressure gradient, stress, gravitation force, interphase momentum exchange due to interfacial forces and mechanical dispersion force.

Conservation of species mass and internal energy must also be solved. The conservation of mass equation for the n^{th} species in the i^{th} phase is

$$\frac{\partial}{\partial t}(\varepsilon_i \rho_i X_{in}) + \nabla \cdot (\varepsilon_i \rho_i \mathbf{u}_i X_{in}) = \nabla \cdot (\mathcal{D}_{gn} \nabla X_{in}) + R_{in} \tag{3}$$

where X_{in} and $\mathcal{D}_{in}$ are the n^{th} species mass fraction and diffusion coefficient of the n^{th} species in the i^{th} phase, respectively. The specific chemistry scheme and corresponding reaction models implemented are used to describe the rate of production/consumption of each chemical species present in the system (R_{in}). The summation of this term over all species present in a given phase becomes a source term in the respective phase continuity equation (see Equation 1).

The conservation of internal energy is presented here in terms of temperature:

$$\varepsilon_i \rho_i C_{pi} \left[\frac{\partial T_i}{\partial t} + \mathbf{u}_i \cdot \nabla T_i\right] = -\nabla \cdot (-\lambda_i \nabla T_i) - \sum_{n=1}^{N_i} h_{in} R_{in} + S_i \tag{4}$$

where, C_{pi} is the i^{th} phase mixture specific heat, T_i is the i^{th} phase temperature, and λ_i is the i^{th} phase thermal conductivity. The first two terms on the right hand side include the conductive

heat flux described by Fourier's Law and changes in internal energy accompanying species formation or destruction due to chemical reactions and phase changes. The last term, S_i, is a general source term which includes interphase heat transfer (convective transfer) and enthalpy transfer accompanying interphase mass transfer (see (Musser, Syamlal, Shahnam, & Huckaby, 2015)). Radiant heat transfer has been neglected. The information needed to close these equations in terms of a gas-liquid solvent absorption application is discussed below.

3. HYDRODYNAMIC CLOSURES

To properly model the hydrodynamics of counter-current gas liquid two phase flow through a packed column, the physics relating to the local film flow operation must be incorporated into the multiphase flow model framework. However, appropriate closure models for this system that capture the micro/meso-scale behavior of the liquid film on a packing material are lacking. The most suitable models currently available in the literature are largely based on co-current trickle bed reactor work. Ideally, small scale CFD simulations, at the level of the film and packing, would also be performed in order to develop high resolution submodels.

3.1 PACKING STRUCTURE

Resolving the complex geometry of the packing structure at device scale is computationally infeasible. Instead the packing structure is replaced with an effective porous media approach. As a result, depicting the intricacies of the packing boundaries and geometrical topology of the packing is avoided while the flow dynamics of the device scale can still be simulated. For random packed beds the porous media type approach has been used with varying level of detail from a mean porosity assigned to the whole bed, to assignment of an axially-averaged radial porosity profile, to a statistical description of the geometry in terms of void fraction profiles. In this effort a uniform mean porosity is assigned to the packing region, a reasonable approximation for representing structured packings.

3.2 CAPILLARY PRESSURE

When two immiscible fluids are in contact with each other, interfacial surface tension may cause the fluids to have different pressures. This discontinuity in pressure is referred to as capillary pressure and may be represented as shown:

$$P_c = P_g - P_l \tag{5}$$

The capillary pressure due to interfacial tension forces will influence wetting and the flow distribution within the packed bed. According to Jiang (Jiang, Khadilkar, Al-Dahhan, & Dudukovic, 2002) in packed beds with large packing elements (20-30-mm Pall/Raschig rings) gravity and inertia are important forces while liquid distribution patterns are not very sensitive to the wettability of the packing surface due to negligible capillary force. In contrast, in trickle beds where the particle sizes are typically in the range of 0.5 to 3mm and all forces may contribute to flow distribution inside the bed. A local constitutive relation must be introduced to account for this difference.

Various correlations have been proposed for capillary pressure including that of Grosser et al. (Grosser, Carbonell, & Sundaresan, 1985) and Attou and Ferschneider (Attou & Ferschneider, 1999). The latter is based on analysis at pore scale corresponding to loss of stability of the liquid film. An additional correction factor for pressure was also incorporated. The capillary pressure model of Grosser et al., which is used in this effort, is expressed through a permeability concept and experimental data in porous media:

$$P_c = \left(\frac{\epsilon}{\kappa}\right)^{\frac{1}{2}} \sigma J(s_l) \tag{6}$$

Here ϵ is the porosity of the packed bed, κ is the permeability, σ is the surface tension, and $J(s_l)$ is the Levertt's J function with s_l being the liquid phase saturation ($s_l = \varepsilon_l/\epsilon$). In multiphase flow through porous media the capillary pressure is often represented by Leverett's function, which is a dimensionless function of liquid saturation describing capillary pressure for media of differing permeability, porosity and wetting properties. In their analysis Grosser fit a portion of the J function data and formulated the permeability of the bed according to their model for the interaction force (an Ergun type relation). The resulting capillary force expression is shown:

$$P_c = \frac{1-\epsilon}{\epsilon d_p}\sqrt{C_1}\sigma\left[0.48 + 0.036\ln\left(\frac{1-s_l}{s_l}\right)\right] \tag{7}$$

By choosing gas phase pressure as the dependent variable the capillary pressure appears through its gradient in the liquid phase momentum balance. This can be seen by introducing the concept of capillary pressure into the liquid phase momentum balance to yield:

$$\begin{aligned}\frac{\partial}{\partial t}(\varepsilon_l\rho_l\mathbf{u}_l) + \nabla\cdot(\varepsilon_l\rho_l\mathbf{u}_l\mathbf{u_l}) \\ = -\varepsilon_l\nabla P_g + \varepsilon_l\nabla P_c + \nabla\cdot(\varepsilon_l\boldsymbol{\tau}_l) + \varepsilon_l\rho_l\mathbf{g} - F_{gl}\left(\mathbf{u}_l - \mathbf{u}_g\right) - F_{sl}\mathbf{u}_l + \mathbf{F}_{Dl}\end{aligned} \tag{8}$$

Assuming the permeability is constant an expression for the gradient in capillary pressure may be obtained as:

$$\nabla P_c = \left(\frac{\epsilon}{\kappa}\right)^{\frac{1}{2}}\sigma\nabla[J(s_l)] = \frac{1-\epsilon}{\epsilon d_p}\sqrt{C_1}\sigma 0.036\left[\frac{-1}{1-\varepsilon_s-\varepsilon_l}(\nabla\varepsilon_s + \nabla\varepsilon_l) - \frac{1}{\varepsilon_l}\nabla\varepsilon_l\right] \tag{9}$$

It has been noted that this model may fail to reproduce the steep rise in capillary pressure as the liquid saturation approaches zero and also may perform questionably for beds characterized by large diameter particles (Lappalainen, Manninen, & Alopaeus, 2009; Lappalainen, Manninen, Alopaeus, Aittamaa, & Dodds, 2009). That said, the model of Grosser et al. does not require empirical parameters and is relatively simple to implement. As a result, this is the model used until evidence indicates refinement is needed.

The capillary term will lead to smearing of the liquid phase front as it travels down the bed and to the diffusion of the liquid phase from regions of higher porosity into regions of lower porosity (Kuzeljevic & Dudukovic, 2012).

3.3 MECHANICAL DISPERSION

While the capillary pressure model will work to disperse the liquid phase it may not be sufficient (Lappalainen, Manninen, & Alopaeus, 2009) to capture the extent of liquid distribution that can occur. Mechanical dispersion is another mechanism for liquid spreading due to the physical variation in the flow path caused by the packing material. In this case variation in the velocity profile at small scale with respect to the mean flow direction is caused by the bed structure. Based on the current capillary pressure model (Equation 9) as the particle size increases the capillary pressure decreases. In contrast, the spread factor due to mechanical dispersion would be expected to increase with particle size. Accordingly separate models are needed for liquid dispersion to capture these two mechanisms (Lappalainen, Manninen, & Alopaeus, 2009).

A rigorous theoretical treatment for mechanical dispersion in the context of the volume averaged two fluid model equations is lacking. However, a few semi-empirical models are available in the literature with a form adequate to introduce dispersion in the present framework (Fourati, Roig, & Raynal, 2013). The model proposed by (Lappalainen, Gorshkova, Manninen, & Alopaeus, 2011; Lappalainen, Manninen, & Alopaeus, 2009) and presented in (Solomenko et al., 2015) is employed which consists of adding a dispersion term to each phase:

$$\mathbf{F}_{Dl} = F_{sl}\mathbf{u}_{Dl} + F_{gl}\left(\mathbf{u}_{Dl} - \mathbf{u}_{Dg}\right) \tag{10}$$

$$\mathbf{F}_{Dg} = F_{sg}\mathbf{u}_{Dg} + F_{gl}(\mathbf{u}_{Dg} - \mathbf{u}_{Dl}) \tag{11}$$

where F_{sl}, F_{sg}, and F_{gl} are the momentum exchange coefficients for the liquid-solid, gas-solid and gas-liquid, respectively. These are discussed below. The drift velocities for the gas ($\mathbf{u}_{Dg}$) and liquid ($\mathbf{u}_{Dl}$) are functions of their saturation and are written in terms of a spread factor (Lappalainen et al., 2011):

$$\mathbf{u}_{Di} = -\frac{S_f}{\varepsilon_i}\left(|\mathbf{u}_i|\nabla\varepsilon_i - (\mathbf{u}_i \cdot \nabla\varepsilon_i)\frac{\mathbf{u}_i}{|\mathbf{u}_i|}\right) \tag{12}$$

where S_f is a spread-factor, which represents a characteristic length of dispersion for a given system and is generally determined from experimental data. The spread factor is defined using the following correlation based on spreading over Raschig rings and Berl saddles of varying size (Lappalainen et al., 2011):

$$S_f[cm] = 0.15\sqrt{\frac{D_p}{cm}} \tag{13}$$

where the quantity D_p is the nominal size of the packing material.

3.4 STRESS

The viscous stress in the fluid phases is described using a Newtonian form requiring a value for effective viscosity (μ_i), which can have contributions from molecular viscosity and the turbulent viscosity. In the latter case, a turbulence model has to be included for multiphase flow in porous media, yielding additional closure equations. Such a model is not considered here and μ_i is simply the molecular viscosity of the fluid. The stress tensor is expressed as

$$\tau_i = 2\mu_i\mathbf{D}_i + \frac{2}{3}\mu_i(\nabla \cdot \mathbf{u_i})\mathbf{I} \tag{14}$$

where μ_i is the viscosity of the i^{th} phase, $\mathbf{D}_i$ is the rate-of-strain tensor $\left(\frac{1}{2}(\nabla \mathbf{u}_i + (\nabla \mathbf{u}_i)^T)\right)$ and $\mathbf{I}$ is the identity tensor.[1]

3.5 INTERACTION FORCE

Coupling between the phases is generally achieved through the pressure and the interphase momentum exchange term (with mass and energy exchange terms also needed for non-isothermal and/or reacting flow). To solve the whole system of governing equations, the interfacial momentum exchange terms also need to be closed in terms of primary variables.

Considerable efforts have been made in the study of the hydrodynamics of trickle bed reactors. Accordingly, a number of constitutive relations have been proposed to describe the phase interactions from empirical approaches to those with a more fundamental physical basis. Several well-known methods include relative permeability type models (Saez & Carbonell, 1985), the slit model (Holub, Dudukovic, & Ramachandran, 1992; Iliuta & Larachi, 1999), and the two fluid interaction model (Attou, Boyer, & Ferschneider, 1999). In this effort the interphase interaction model of Attou et al. (Attou et al., 1999) is employed. This model is derived assuming gas-liquid flow through a fixed bed of solid particles. The packing surface is completely covered by the liquid film and the gas flows in the central zone so that the gas and liquid phases are completely separated by a smooth interface. With this depiction the mathematical form of the interaction forces as they relate to the local microscopic forces are derived directly from the momentum balance equations. These are then closed by considering the Kozeny-Carman equation, or more aptly the Ergun relation which accounts for both viscous and inertia contributions, applied to each fluid and taking into account the two phase pattern. Note that the pressure drop in packed beds is often correlated with Ergun's relation or a variation thereof, and so formulation of the interphase coupling terms are also often based on a similar approach.

For ease of implementation, the interphase coupling terms proposed by Attou et al (Attou et al., 1999) are rewritten here in terms of interstitial velocities and phase volumes (instead of superficial velocities and saturation) (Gunjal & Ranade, 2007). Here, the tortuosity factor (inversion of liquid saturation) was omitted from the liquid-solid interaction term. The correlations below provide a mechanism to demonstrate a solvent absorption model, and may easily be replaced by a more suitable model depending upon the application of interest.

$$F_{gl} = \varepsilon_g \left(\frac{C_1 \mu_g (1-\varepsilon_g)^2}{\varepsilon_g^2 d_p^2} \left[\frac{\varepsilon_s}{1-\varepsilon_g} \right]^{\frac{2}{3}} + \frac{C_2 \rho_g (1-\varepsilon_g) |\mathbf{u}_g - \mathbf{u}_l|}{\varepsilon_g d_p} \left[\frac{\varepsilon_s}{1-\varepsilon_g} \right]^{\frac{1}{3}} \right) \tag{15}$$

[1] MFIX assumes the fluid phase bulk viscosity (second viscosity, volume viscosity) is zero. Recall, the bulk viscosity is the proportionality constant relating pure volumetric-rate-of strain to the normal stress.

$$F_{sg} = \varepsilon_g \left(\frac{C_3 \mu_g (1-\varepsilon_g)^2}{\varepsilon_g^2 d_p^2} \left[\frac{\varepsilon_s}{1-\varepsilon_g} \right]^{\frac{2}{3}} + \frac{C_4 \rho_g (1-\varepsilon_g) |\mathbf{u}_g|}{\varepsilon_g d_p} \left[\frac{\varepsilon_s}{1-\varepsilon_g} \right]^{\frac{1}{3}} \right) \quad (16)$$

$$F_{sl} = \varepsilon_l \left(\frac{C_5 \mu_l \varepsilon_s^2}{\varepsilon_l^2 d_p^2} + \frac{C_6 \rho_l \varepsilon_s |\mathbf{u}_l|}{\varepsilon_l d_p} \right) \quad (17)$$

Here C_1 - C_6 are constants, and other quantities are as before. The subscripts $i = g, l$ and s refer to the gas, liquid and solids (packing) phase respectively. In this work the values of $C_{1,3,5}$ and $C_{2,4,6}$ are taken by default as 180 and 1.8, respectively. The quantity d_p is referred to as the surface-volume equivalent sphere diameter of the particles ($d_p = 6V_p/S_p$ where V_p and S_p are the volume and area of the particle respectively). For the gas phase the Ergun equation is modified for gas-liquid flow with an apparent particle size due to liquid film at the surface. For the liquid phase the liquid flows over the solid surface through a bed with porosity reduced by gas hold-up. The interfacial force on the gas phase involves the drag force acting on the gas due to relative motion between the fluids as well as the force that arises from the gas pushing on the packing surface through the liquid layer (due to the torturous pattern and successive cross-section area changes of the interstitial flow path). The interfacial force on the liquid phase also involves the drag force acting on the liquid phase resulting from slip motion between the fluids as well as the force on the liquid due to the shear of the liquid layer along the packing surface. Note that the force by which the gas phase pushes the liquid film against the packing surface is not included in the resulting interaction force on the liquid because it cancels with the equal and opposed reacting force exerted by the packing surface on the liquid film.

As noted by Kuzeljevic and Dudukovic (Kuzeljevic & Dudukovic, 2012) the phase interaction closures will reduce the speed at which the liquid front travels and increase the liquid saturation of the front.

4. HEAT AND MASS TRANSFER MODEL CLOSURES

In the case of gas absorption, mass and heat transfer occur simultaneously. The chemical reaction rates will depend strongly on temperature as will the vapor-liquid equilibrium point. So temperature variation within the column is an important factor in design of a gas absorption process (Pandya, 1983). To develop a comprehensive model for solvent absorption also requires some description of the underlying mechanism by which the absorption takes place. That is, the model must encompass mass transfer of CO_2 from the bulk gas to the solvent, solution reactions between CO_2 and solvent species, and the associated kinetic regimes.

4.1 SOLVENT ABSORPTION CHEMISTRY

Monoethanolamine (MEA) is a common chemical solvent and the focus of this study. The reactions between CO_2 and amines are complex and still not fully understood despite significant industrial application. The majority of work to date assumes the reaction proceeds through a zwitterion mechanism (Danckwerts, 1979), although evidence also supports a termolecular mechanism (Aboudheir, Tontiwachwuthikul, Chakma, & Idem, 2003; Crooks & Donnellan, 1989). In the zwitterion mechanism, the reaction between CO_2 and primary (e.g., MEA) and secondary amines is represented in a two-step process (Aboudheir et al., 2003; Danckwerts, 1979; Versteeg, van Dijck, & van Swaaij, 1996). First, reaction of MEA (R_1R_2NH) with CO_2 occurs to form a zwitterion intermediate[2] ($R_1R_2NH^+COO^-$). The notation R refers to a functional group, and they are defined here for MEA as $R_1 = -C_2H_2OH$ and $R_2 = -H$. The zwitterion is subsequently deprotonated by some base, B, to form a carbamate ($R_1R_2NCOO^-$). Any base such as (R_1R_2NH, OH^-, H_2O, HCO_3^- and CO_3^{--}) may also contribute to the deprotonation of the zwitterion.

$$CO_2(l) + R_1R_2NH \overset{k_2,k_{-1}}{\longleftrightarrow} R_1R_2NH^+COO^- \qquad \textbf{Zwitterion formation} \tag{18}$$

$$R_1R_2NH^+COO^- + B \overset{k_b,k_{-b}}{\longleftrightarrow} R_1R_2NCOO^- + BH^+ \qquad \textbf{Formation of Carbamate} \tag{19}$$

The overall forward rate of reaction for this mechanism is given by (Caplow, 1968; Danckwerts, 1979) (see also discussion by (Versteeg et al., 1996)) as follows:

$$r_{CO_2-MEA} = \frac{[CO_2][R_1R_2NH]}{\frac{1}{k_2}+\frac{k_{-1}}{k_2\sum k_b[B]}} \tag{20}$$

Here, k_2 and k_{-1} are the forward and reverse rate constants in Reaction 18 and k_b is the forward rate constant for the contribution of base B to Reaction 19. A common simplification of Equation 20 results from the assumption that the zwitterion is completely deprotonated before it

[2] In aqueous MEA solutions, CO_2 can also react directly with OH^- to form bicarbonate (HCO_3^-). However, the concentration of OH^- ions is almost always very small in solution 24, and the rate of consumption of CO_2 via this pathway is neglected.

can revert to CO_2 and R_1R_2NH. In this case, the overall rate of reaction becomes first order with respect to both CO_2 and MEA in terms of molar concentrations[3]:

$$r_{CO_2-MEA} = k_2[CO_2][R_1R_2NH]. \tag{21}$$

Furthermore, in small to intermediate loading regions ($mol\ CO_2/mol\ R_1R_2NH \lesssim 0.5$), the concentration of base ions (OH^-, HCO_3^- and CO_3^{--}) will generally be small, so that their contribution to the deprotonation of the zwitterion can be considered negligible . Base B in Reaction 19 then becomes R_1R_2NH and the overall conversion of CO_2 may be approximated as the following single step irreversible kinetic reaction:

$$CO_2(l) + 2R_1R_2NH \overset{k_2}{\rightarrow} R_1R_2NCOO^- + R_1R_2NH_2^+ \qquad \textbf{Overall conversion of } \boldsymbol{CO_2(l)} \tag{22}$$

This simplification can probably be considered valid under absorber conditions involving relatively low CO_2 loading so that the zwitterion formation is rate controlling and the concentration of the bicarbonates and carbonates is not significant.

The second order reaction rate constant (k_2) is well characterized by a rate expression given by Hikita (Hikita, Asai, Ishikawa, & Honda, 1977)

$$\log(k_2) = 10.99 - \frac{2152}{T}. \tag{23}$$

Here, k_2 has units $\frac{liter}{gmol.s}$ and T is the absolute temperature in units $Kelvin$.

A number of parallel equilibrium reactions accompany this rate controlled conversion of CO_2 in amine solutions, which are responsible for determining the bulk solution composition. They are described in detail by Aboudheir (Aboudheir et al., 2003) and Hiwale (Hiwale, Hwang, & Smith, 2012). Of these, the following five are thought to be important for loaded MEA solutions when deprotonation of the zwitterion by species other than MEA can be neglected:

$$R_1R_2NCOO^- + H_2O \overset{K_1}{\leftrightarrow} R_1R_2NH + HCO_3^- \qquad \textbf{Reversion of carbamate} \tag{24}$$

$$CO_2(l) + 2H_2O \overset{K_2}{\leftrightarrow} HCO_3^- + H_3O^+ \qquad \textbf{Dissociation of } \boldsymbol{CO_2} \tag{25}$$

$$HCO_3^- + H_2O \overset{K_3}{\leftrightarrow} CO_3^{--} + H_3O^+ \qquad \textbf{Dissociation of } \boldsymbol{HCO_3^-} \tag{26}$$

$$R_1R_2NH_2^+ + H_2O \overset{K_4}{\leftrightarrow} R_1R_2NH + H_3O^+ \qquad \textbf{Dissociation of } \boldsymbol{R_1R_2NH_2^+} \tag{27}$$

$$2H_2O \overset{K_5}{\leftrightarrow} H_3O^+ + OH^- \qquad \textbf{Ionization of water} \tag{28}$$

[3] This simplification seems to be valid for MEA, but not necessarily for other amine based solvents, where the second term in the denominator of Equation 20 can be large (Danckwerts, 1979).

Each Reaction 24-28 above represents an independent equilibrium constraint on the bulk composition. Equilibrium constants are defined on a molarity scale as shown:

$$K_1 = [R_1R_2NH][HCO_3^-]/[R_1R_2NCOO^-] \quad (29)$$

$$K_2 = [HCO_3^-][H_3O^+]/[CO_2] \quad (30)$$

$$K_3 = [CO_3^{--}][H_3O^+]/[HCO_3^-] \quad (31)$$

$$K_4 = [R_1R_2NH][H_3O^+]/[R_1R_2NH_2^+] \quad (32)$$

$$K_5 = [H_3O^+][OH^-] \quad (33)$$

Here, the notation [ ] indicates the equilibrium molar concentration of a chemical species in the bulk liquid. Based on the work of (Aboudheir et al., 2003), the functional dependence of K_1, K_2, K_3, K_4, K_5 on temperature is of the form,

$$ln(K_i) = A + \frac{B}{T} + C * ln(T). \quad (34)$$

The constants A, B, C are reproduced in Table 1 along with their original source[4].

Table 1. Coefficients of the Equilibrium Constant, K_i, in Equation 34 for Reactions 24-28

	A	B	C	Source
$K_1(mol/dm^3)$	6.69425	-3090.83	0.0	(Kent & Eisenberg, 1976)
$K_2(mol/dm^3)$	235.482	-12092.1	-36.7816	(Edwards, Maurer, Newman, & Prausnitz, 1978)
$K_3(mol/dm^3)$	220.067	-12431.7	-35.4819	(Edwards et al., 1978)
$K_4(mol/dm^3)$	-3.3636	-5858.11	0.0	(Kent & Eisenberg, 1976)
$K_5(mol/dm^3)^2$	140.932	-13445.9	-22.4773	(Edwards et al., 1978)

4.1.1 Reaction Model

It is only when the CO_2 enters the liquid phase that it can react with the MEA solution. Therefore, the overall rate of absorption needs to account for the mass transfer resistance and enhancement due to chemical reactions. Accordingly, the mass transfer from the gas bulk into

[4] The units reported for these coefficients are mixed in the literature, with some authors using molality (mol/kg water) and some molarity (gmol/liter solution). Here, we follow the convention of Aboudheir [22] and convert all units to molarity ($mol/dm^3\ solution$), which is applicable for dilute solutions.

the gas boundary layer, across the gas-liquid interface and from the interface through the liquid reaction boundary layer and finally into the liquid bulk need to be established. Recall that the Eulerian-Eulerian approach does not accomplish interface tracking and so is unable to capture either the wetting characteristics at the gas-liquid interface or the distribution of chemical species within the boundary layer(s). Such information must be introduced through appropriate modeling. Many different approaches to modeling mass transfer with chemical reaction can be found in the literature. In this effort film theory is used (see (Levenspiel, 1999)).

In the two film model it is assumed that resistance to mass transfer occurs in two thin films adjacent to the phase interface. Mass transfer within the films occurs by steady state molecular diffusion. Outside the films, in the gas/liquid bulk, mixing is sufficiently high so that only diffusion transport normal to the interface occurs. For amine solvents in absorber conditions, the overall conversion of CO_2 (Reaction 22) is fast enough to occur only in the liquid film. Outside this region, in the liquid bulk, the nine liquid species are in chemical equilibrium and constraints 29-33 can be used to determine their bulk concentrations (see discussion on implementation next section).

Following the work of Pandya (Pandya, 1983), the mass flux of CO_2 across the gas-liquid interface at steady state, N_{CO_2}, can be presented in terms of a mass transfer coefficient and driving force. The general forms of the flux equations are shown here.

$$N_{CO_2} = k_g a\left(p_{CO_2} - p_{CO_2}^{\text{interface}}\right) \tag{35}$$

$$N_{CO_2} = k_l^{\circ} a \mathrm{E}\left([CO_2]^{interface} - [CO_2]\right) \tag{36}$$

where k_g and k_l^o are the physical mass transfer coefficients of the CO_2 species in the gas and liquid phase, respectively, a is the interfacial surface area per unit volume of bed, $[CO_2]$ and $[CO_2]^{interface}$ are the molar concentration of CO_2 in the liquid bulk and interface, p_{CO_2} and $p_{CO_2}^{\text{interface}}$ are the partial pressure of CO_2 in the gas bulk and interface, and E is the enhancement factor due to chemical reaction.

Through a combination of the two flux equations (Equations 35 and 36) and using Henry's law for vapor liquid equilibrium, an expression for the interfacial concentration of CO_2 is obtained as follows:

$$p_{CO_2}^{\text{interface}} = \frac{p_{CO_2} + \frac{k_l^{\circ} E}{k_g}[CO_2]}{1 + \frac{k_l^{\circ} E}{k_g H}} \tag{37}$$

Here, H is Henry's constant $\left([CO_2]^{\text{interface}} = \frac{p_{CO_2}^{\text{interface}}}{H}\right)$. Using this expression for the partial pressure at the interface, the flux of CO_2 from the gas to liquid phase is described. To evaluate this expression requires knowledge of the physical-chemical properties of the fluids involved in the process including gas and liquid phase mass transfer coefficients, interfacial area, density, viscosity, solubility, and diffusivity.

The acceleration of mass transfer due to chemical reaction in the interfacial region is accounted for by what is known as the enhancement factor. The functional dependency of the enhancement factor is determined by the specific kinetic reaction taking place in the liquid film. Here the enhancement factor for a system with second-order irreversible reaction kinetics proposed by Wellek (Wellek, Brunson, & Law, 1978) is used.

$$\mathrm{E} = 1 + \frac{1}{\left[\frac{1}{(\mathrm{E_i} - 1)^{1.35}} + \frac{1}{(\mathrm{E_1} - 1)^{1.35}}\right]^{\frac{1}{1.35}}} \tag{38}$$

$\mathrm{E_i}$ and $\mathrm{E_1}$ are dimensionless parameters for different limiting conditions of an infinitely fast reaction and pseudo-first-order reaction, respectively. For the CO_2–MEA system these quantities are defined as follows:

$$\mathrm{E_i} = 1 + \left(\frac{[R_1R_2NH]}{2[CO_2]^{\mathrm{interface}}}\right)\left(\frac{\mathcal{D}_{l,MEA}}{\mathcal{D}_{l,CO_2}}\right) \tag{39}$$

$$\mathrm{E_1} = \frac{\mathrm{Ha}}{\tanh(\mathrm{Ha})} \tag{40}$$

where $[R_1R_2NH]$ is the concentration of MEA and $\mathcal{D}_{l,CO_2}$ and $\mathcal{D}_{l,MEA}$ are the diffusivity of CO_2 and MEA in the liquid phase, respectively. The first order enhancement factor is a function of the dimensionless number known as the Hatta number (Ha). The Hatta number compares the ratio between the maximum chemical conversion in the film and the maximum diffusion flux through the film. In the case of a second order reaction it is defined as:

$$\mathrm{Ha} = \frac{\sqrt{\mathcal{D}_{l,CO_2}k_2[R_1R_2NH]}}{k_l^o} \tag{41}$$

where k_2 is the kinetic rate constant given in Equation 23. When all the reactions occur in the film the Ha is much greater than one. The fast reaction regime corresponds to the Hatta number ranging from around 3 to 5 (Razi, Bolland, & Svendsen, 2012).

4.1.2 Reaction Model: Parameters

To evaluate the reaction model above requires information on the physicochemical properties, discussed shortly, as well as on the mass-transfer coefficients and gas-liquid contact area. A number of empirical, and semi-theoretical models for predicting mass transfer in packed columns have been published in the literature (e.g., (Razi et al., 2012; Wang, Yuan, & Yu, 2005)). Complicating physics (interfacial behavior, complex geometry/structure effects) related to this system are accommodated into the model framework through these terms. The correlations will depend on packing type and system conditions, and therefore, are not universally applicable. That is, these correlations will have different limitations restricting their suitability for application.

In this effort the empirical correlations of Onda (Onda, Takeuchi, & Okumoto, 1968) are used for predicting the interfacial area and gas and liquid-side mass transfer coefficients:

$$\frac{a_w}{a_t} = 1 - \exp\left(-1.45 \frac{\sigma_c^{0.75} g^{0.05} L^{0.4}}{\sigma^{0.95} a_t^{0.35} \mu_l^{0.1} \rho_l^{0.1}}\right) \tag{42}$$

$$k_l^o = 0.0051 \left(\frac{L}{a_w \mu_l}\right)^{\frac{2}{3}} \left(\frac{\mu_l}{\rho_l \mathcal{D}_{l,s}}\right)^{-\frac{1}{2}} (a_t D_p)^{0.4} \left(\frac{\mu_l g}{\rho_l}\right)^{\frac{1}{3}} \tag{43}$$

$$k_g = 5.23 \left(\frac{G}{a_t \mu_g}\right)^{0.7} \left(\frac{\mu_g}{\rho_g \mathcal{D}_{g,s}}\right)^{\frac{1}{3}} (a_t D_p)^{-2.0} \left(\frac{a_t \mathcal{D}_{g,s}}{RT}\right) \tag{44}$$

where a_w is the wetted surface area of packing per unit volume of bed, a_t is the total surface area of packing per unit volume of bed (also known as the specific area), R is the universal gas constant , T is the absolute temperature , D_p is the nominal size of the packing material, σ_c is the surface tension of the packing material, L is the superficial mass velocity of the liquid $(L = u_l \rho_l \varepsilon_l)$, G is the superficial mass velocity of the gas $\left(G = u_g \rho_g \varepsilon_g\right)$, $\mathcal{D}_{g,s}$ is the diffusivity of the solute species in the gas phase, $\mathcal{D}_{l,s}$ is the diffusivity of the solute in the liquid phase. The other symbols are as noted earlier. In their work, and here, the wetted surface of the packing is assumed identical to the effective interfacial area (i.e., $a = a_w$). It is worth noting that these correlations were developed based on random packed columns. That said, these correlations simply provide a mechanism to demonstrate this solvent absorption model, and as in the case of other closure quantities, may easily be replaced by a more suitable model depending upon the application of interest. The values of a_t, D_p ,and σ_c will depend on the specific packing material.

4.2 HEAT TRANSFER MODEL

To evaluate the thermal balance equations (Equation 4) for the gas and liquid phases requires constitutive relations to describe the different mechanisms of energy transport. As noted earlier the main heat transfer mechanisms in the flow are interphase heat transfer (convective transfer) and enthalpy transfer accompanying interphase mass transfer. Closures for these are discussed below in more detail.

Note that the change in internal energy accompanying species formation or destruction due to chemical reactions and phase changes (the second term on the right hand side of Equation 4) requires that the specific enthalpy of each species be evaluated. This is generally calculated by combining the heat of formation with the integration of the specific heat of that species from the reference temperature to that phase temperature.

4.2.1 Interphase Heat Transfer (Convective)

An expression for interphase heat transfer is assumed to be function of the temperature difference. At this time only interphase heat transfer between the gas and liquid phase and the gas and solids phase (packing material) is described as follows. No heat transfer is defined between the liquid and packing material.

$$S_{g,convl} = \gamma_{gl} A (T_l - T_g) \tag{45}$$

$$S_{g,convs} = \gamma_{gs} A (T_s - T_g) \tag{46}$$

Here $\gamma_{gl}$and γ_{gs} are the coefficients of heat transfer between gas and liquid and gas and packing, respectively, and A represents the area put unit volume of bed available for the indicated heat transfer. With respect to gas-liquid heat transfer A corresponds to a, the interfacial area per unit volume of bed, which in equated to a_w the wetted area. For gas-solid heat transfer A is taken as a_t, which is the specific area or total area of packing per unit volume of bed. Neither is fully accurate. The interphase heat transfer is added to the gas phase internal energy equation (Equation 4 for $i = g$) through the general source term S_g. The heat transfer between the gas and liquid (Equation 45) is subtracted from the liquid phase internal energy equation (Equation 4 for $i = l$) through the general source term S_l.

The heat-transfer coefficients are typically related to the Nusselt number (Nu), which is defined as the ratio of convective to conductive heat transfer across a boundary:

$$\mathrm{Nu}_{gk} = \frac{\gamma_{gk} L}{\lambda_g} \tag{47}$$

where λ_g is the thermal conductivity of the gas phase, γ_{gk} is the heat transfer coefficient between the gas phase and phase *k* (where *k* = liquid or solid) and *L* is the characteristic length.

The Ranz-Marshal (Ranz & Marshall, 1952) correlation for the Nusselt number is used to describe the heat transfer between the gas and liquid phase:

$$\mathrm{Nu}_{gl} = 2 + 0.6 \mathrm{Re}_{gl}^{1/2} \mathrm{Pr}_g^{1/3} \tag{48}$$

where Re_{gl} and Pr_g are the Reynolds and Prandlt numbers, defined below, respectively. This correlation was developed for fluid flow around a water drop (sphere). In this effort, the fluid is taken as the gas phase and the sphere represents the liquid phase around the packing material. The Reynolds number is defined based on gas phase physical properties, the superficial velocity that represents the gas-liquid relative motion ($\mathbf{j}_r$) and an effective diameter of the liquid phase (d_{pl}). The superficial relative velocity is re-written in terms of interstitial gas and liquid velocity and volume fraction as $\mathbf{j}_r = \varepsilon_g (\mathbf{u}_g - \mathbf{u}_l)$ (Attou et al., 1999). Using this information the Reynolds number is defined as shown:

$$\mathrm{Re}_{gl} = \frac{\rho_g \varepsilon_g |\mathbf{u}_g - \mathbf{u}_l| d_{pl}}{\mu_g} \tag{49}$$

Following (Attou et al., 1999), an effective particle diameter (d_{pl}) that is larger than the actual diameter of the packing material and accounts for the wetting of the liquid film on the packing material is defined as:

$$d_{pl} = \left[\frac{1 - \varepsilon_g}{1 - \epsilon}\right]^{1/3} d_p \tag{50}$$

The Prandlt number is defined below for fluid phase *i* (where *i* = gas or liquid phase):

$$\mathrm{Pr}_i = \frac{C_{pi}\mu_i}{\lambda_i} \tag{51}$$

For Nu_{gl} the representative length is taken as the effective particle diameter ($L = d_{pl}$). Combining these relations the heat transfer coefficient between the gas and solids phase may be identified.

The Nusselt correlation by Gunn (Gunn, 1978) is used to describe the heat transfer between the gas and packing material (Nu_{gs}). This empirical correlation is developed based on continuous single phase fluid and is a function of bed porosity. In the current effort the porosity is re-interpreted using an effective porosity that is smaller than the actual global porosity (Attou et al., 1999). Therefore, the correlation is written as follows for gas-solids heat transfer:

$$\begin{aligned}\mathrm{Nu}_{gs} = {} & \left(7 - 10\varepsilon_g + 5\varepsilon_g^2\right)\left(1 + 0.7\mathrm{Re}_{sg}^{0.2}\mathrm{Pr}_g^{1/3}\right) \\ & + \left(1.33 - 2.4\varepsilon_g + 1.2\varepsilon_g^2\right)\mathrm{Re}_{sg}^{0.7}\mathrm{Pr}_g^{1/3}\end{aligned} \tag{52}$$

where $\mathrm{Re}_{sg}$and Pr_g are the Reynolds and Prandlt numbers, respectively. The Prandlt number is as defined previously. The Reynolds number is defined as:

$$\mathrm{Re}_{si} = \frac{\rho_i \varepsilon_i |\mathbf{u}_i| d_p}{\mu_i} \tag{53}$$

The representative length (L) is given by d_p. This correlation may also be used to define the liquid-packing heat transfer (Nu_{ls}), where the subscript *g* is replaced with subscript *l*. However, this component is currently neglected due to limitations in MFIX.

4.2.2 Interphase Heat Transfer by Interphase Mass Transfer

Closure for interphase enthalpy transfer accompanying interphase mass transfer in the context of the multiphase Eulerian-Eulerian approach is described in detail by Musser (Musser et al., 2015). The proposed closure requires the specific enthalpies of the relevant species involved. As noted earlier this information is already needed to describe the change in internal energy accompanying species formation or destruction. Therefore no additional property information is required to evaluate the interphase enthalpy transfer due to mass transfer. As explained later, this detailed calculation may be superseded by explicitly defining a 'heat of reaction' for a given reaction and indicating how this energy is partitioned between the associated phases.

5. IMPLEMENTATION NOTES

A model for counter current gas-liquid flow through a packed column is implemented using MFIX's two fluid approach. MFIX is traditionally used for modeling gas-solids flows wherein the gas phase is treated as the primary continuous phase (marked phase 0) and any additional solids are treated as secondary continuous solids phases (marked as phases 1 on up accordingly). To model solvent absorption three continuous phases are employed. The gas is modeled as phase 0. Two additional continuous 'solids' phases are employed to model the liquid and packing material. The liquid phase is taken as 'solids' phase 1 while the packing material is taken as 'solids' phase 2. To invoke the form of the governing equations presented earlier the keyword `ISHII` must be specified to `.TRUE.` in the input file.

The additional physics and chemistry are primarily implemented in user-defined modules to minimize interference with MFIX. A list of all modified files is provided in Table 2 with additional details covered in the sections that follow. To invoke the user files in MFIX the keyword `CALL_USR=.TRUE.` must be set in the input file.

Table 2. Source Code Modifications and UDF Overview

usr_mod.f,	User defined global variables, functions and subroutines. Contains most of the models needed to specify the physio-chemical properties and transport coefficients.
usrnlst.inc, usr_init_namelist.f	User defined keywords that may be specified in input file and their initialization.
usr0.f.	User input checks and allocation/initialization of some user defined global variables.
usr1.f	Master subroutine to direct calculation of chemical equilibrium depending on the simulation setup.
usr2.f	Master subroutine to direct calculations of surface tension and fractional wetted area depending on the simulation setup: σ_l and a_w/a_t
usr_rates.f	User defined chemical reactions.
usr_sources.f	Subroutines to calculate capillary pressure terms and mechanical dispersion terms.
usr_drag.f	Subroutine to calculate gas-solid and gas-liquid interphase interaction terms: F_{gs} and F_{gl}
usr_properties.f: usr_prop_fss	Liquid-solid interphase interaction: F_{ls}
usr_properties.f: usr_prop_difl	Liquid phase diffusivity: $\mathcal{D}_{l,n} = \mathcal{D}_l$

usr_properties.f: usr_prop_kl	Liquid phase conductivity: λ_l
usr_properties.f: usr_prop_gama	Heat transfer coefficients: γ_{gl} and γ_{gs}
usr_properties.f: usr_prop_mus	Liquid phase viscosity: μ_l
usr_properties.f: usr_prop_ros	Liquid phase density: ρ_l

In addition, several new keywords are introduced in the input file as summarized here in Table 3 and discussed in the relevant sections below. These new keyword terms are included through the files usr_mod.f, usr_init_namelist.f and usrnlst.inc.

Table 3. New User Input Keywords for Input File

Keyword [default value]	Type	Description
`solvent_absorption [.false.]`	L	Solvent absorption module features. If set to false (default), many of the user defined property functions will not be accessible.
`cap_press_type [undefined_c]`	C	Capillary pressure model. Valid options include `'GROSSER_1988'`. This is based on the model of Grosser et al. (Grosser et al., 1985). If left undefined (default), capillary pressure is not modelled.
`usr_drag_type [undefined_c]`	C	Phase interaction (drag) model. Valid options include `'ATTOU_99_MOD'`, `'ATTOU_99'`, `'LAPPALAINEN_09_MOD'`, `'LAPPALAINEN_09'`, and `SOLOMENKO_15`. These are based on the modified and original model of Attou et al. (Attou et al., 1999), the modified and original model of Lappalainen et al. (Lappalainen, Manninen, Alopaeus, et al., 2009), and of Solomenko et al. (Solomenko et al., 2015), respectively. See code for details. If left undefined (default), the simulation will abort. See also `apply_waf`.
`mech_dispersion [.false.]`	L	Mechanical dispersion model. If set to `false` (default), mechanical dispersion is not modelled.
`spread_factor [undefined]`	DP	Value of the spread factor used by the mechanical dispersion model. Units length. If left undefined (default), it is calculated based on model setup described earlier.

enhancement_factor [undefined]	DP	Value of the enhancement factor. Used in calculation of mass transfer of CO_2. Nondimensional. If left undefined (default), it is calculated based on model of Wellek (Wellek et al., 1978).
wetarea_type [undefined]	C	Fractional wetted area model defined as the wetted area of the packing per unit volume of bed. Nondimensional. Valid options include 'ONDA_68', 'LAPPALAINEN_08', and 'CONSTANT'. These are based on the model of Onda et al. (Onda et al., 1968), and Lappalainen et al. (Lappalainen, Alopaeus, Manninen, & Aittamaa, 2008). Specifying 'CONSTANT' also requires specifying the keyword wetareafrac0. If left undefined (default), the fractional wetted area is set to 1.
wetareafrac0 [undefined]	DP	Required keyword only if wetarea_type='CONSTANT'. Defines the value of the fractional wetted area. Nondimensional. If left unspecified (default) and wetarea_type='CONSTANT', the simulation will abort.
apply_waf [.false.]	L	Runtime flag that determines whether to apply a fractional wetted area term to the interphase interaction terms. If set to .false. no fractional wetted area factor is employed. This should be set to .true. for some interaction models to remain consistent with their published form.
sa_pack [undefined]	DP	Specific area of the packing – surface area of packing per unit volume of bed. Units length^2·length^{-3}.
d_pack [d_p0(2)]	DP	Nominal size of packing. Units length. Used in calculation of gas- and liquid- side mass transport coefficients, and if needed, in calculation of the spread factor. This quantity is introduced to permit differentiation between nominal packing size and surface-volume equivalent sphere diameter.
omega_pack [undefined]	DP	Critical surface tension of packing – surface energy. Units force·length^{-1} or mass·time^{-2}. Used in calculation of liquid side mass transport coefficient.

omega_l0 [undefined]	DP	Liquid surface tension. Units force·length^{-1} or mass·time^{-2}. If left undefined (default), surface tension is calculated based on model setup described earlier.
ABSORBER_CHEM_TYPE [undefined_c]	C	Required keyword. Determines the chemistry scheme used for coupled mass transfer and chemical reaction in the liquid phase. Valid options are described in more detail below and include 'SINGLE_STEP', 'EQUILIBRIUM_SEGREGATED', and 'EQUILIBRIUM_COUPLED'.
C [undefined]	DP	User defined constants. The following constants are specifically defined in this module as indicated here. If left undefined (default), each will be assigned a value of 1. C(1) = calibration factor for Henry's constant (H_{new} =C(1)H). C(2) = calibration factor for gas phase mass transfer coefficient ($k_{g,new}$ =C(2)k_g). C(3) = calibration factor for liquid phase mass transfer coefficient ($k^o_{l,new}$ =C(3)k^o_l). C(5) = calibration factor for viscous term in gas-liquid interaction model ($C_{1,new}$ =C(5)C_1). C(6) = calibration factor for inertial term in gas-liquid interaction model ($C_{2,new}$ =C(6)C_2). C(7) = calibration factor for viscous term in gas-solids interaction model ($C_{3,new}$ =C(7)C_3). C(8) = calibration factor for inertial term in gas-liquid interaction model ($C_{4,new}$ =C(8)C_4). C(9) = calibration factor for viscous term in liquid-solids interaction model ($C_{5,new}$ =C(9)C_5). C(10) = calibration factor for inertial term in liquid-solids interaction model ($C_{6,new}$ =C(10)C_6). C(11) = forward reaction rate constant for carbamate reversion in units time^{-1} ($k_{1,fwd}$ =C(11)) with $K_1 = k_{1,fwd}/k_{1,rvs}$.

		C(12) = forward reaction rate constant for dissociation of dissolved CO_2 in units time^{-1} ($k_{2,fwd}$ =C(12)) with $K_2 = k_{2,fwd}/k_{2,rvs}$. C(13) = forward reaction rate constant for dissociation of bicarbonate in units time^{-1} ($k_{3,fwd}$ =C(13)) with $K_3 = k_{3,fwd}/k_{3,rvs}$. C(14) = forward reaction rate constant for dissociation of protonated MEA in units time^{-1} ($k_{4,fwd}$ =C(14)) with $K_4 = k_{4,fwd}/k_{4,rvs}$. C(15) = forward reaction rate constant for ionization of water in units amount of substance length^{-3}·time^{-1} ($k_{5,fwd}$ =C(15)) with $K_5 = k_{5,fwd}/k_{5,rvs}$.

5.1 HYDRODYNAMIC MODEL & PARAMETERS

As noted earlier, the primary information of the structure of the gas-liquid interface becomes lost in such an approach and must be introduced again through the closure models noted earlier. These interaction models are not readily available in MFIX and therefore had to be incorporated using the appropriate user hooks.

The interaction terms are included in the files usr_drag.f and usr_properties.f, which are invoked by specifying the appropriate keyword as noted in the MFIX user guide. Specifically, the following keywords must be set in the input file: DRAG_TYPE='USER_DRAG' and USR_FSS(1)=.TRUE.. In addition, a new keyword, USR_DRAG_TYPE, must be set to specify the interaction model. Several options are available as indicated in Table 3. The interphase interaction formulations outlined in Equations 15-17 correspond to option 'ATTOU_99_MOD'. This model depends on the quantity d_p, which as noted earlier represents a surface-volume equivalent sphere diameter of the particles. In the MFIX implementation the quantity d_p is assigned to the diameter of 'solids' phase 2 that is specified in the input file (i.e., d_p =d_p0(2)).

The capillary pressure term (Equation 9) appears as a new source term in the momentum equations. The capillary pressure term is included in the file usr_sources.f, which is invoked by specifying the appropriate keyword as noted in the MFIX user guide. Specifically, the following keywords must be set in the input file: USR_SOURCE(3)=.TRUE., USR_SOURCE(4)=.TRUE., and USR_SOURCE(5)=.TRUE.. In addition, a new keyword must be set to indicate the capillary pressure model: CAP_PRESS_TYPE='GROSSER_1988'. To evaluate this correlation requires, among others, a value for the surface tension (σ). To specify this value a new keyword were introduced into MFIX (see Table 3) as σ_l =omega_l0. This may be set in the input file. If left undefined then the surface tension model indicated in Table 5, below, is used. For a non-reacting flow simulation this model will return a value for water.

The mechanical dispersion term appears as a new source term in the momentum equations. Like capillary pressure, the mechanical dispersion term is included in the file usr_sources.f. Accordingly, the following keywords must be set in the input file if they have not already: `USR_SOURCE(3)=.TRUE.`, `USR_SOURCE(4)=.TRUE.`, and `USR_SOURCE(5)=.TRUE.`. To invoke this force `MECH_DISPERSION=.TRUE.` must be set. The spread factor (Equation 13) in the mechanical dispersion formulations (Equations 10 and 11) may be explicitly set in the input file through the keyword `spread_factor` (see Table 3). If it is left unspecified, then by default Equation 13 is used to calculate a value. This formula depends on the quantity D_p, which represents the nominal packing size. The nominal packing size may be specified using the new keyword `dp_pack` (see Table 3). If left unspecified, the nominal size of the packing material is also simply assigned to the diameter of 'solids' phase 2 (i.e., D_p =`d_p0(2)`).

To fully close the continuity and momentum balance equations (Equations 1 and 2) requires a value for the density and viscosity of the gas and liquid phases. Depending on the phase density may be specified either as a constant value in the input file, or as a calculated value using either a default model or through a customized user routine in the file usr_properties.f. In MFIX, the default model for the gas phase density is that of an ideal gas (Syamlal et al., 1993). Generally, MFIX requires that the liquid phase density be specified as a constant in the input file. To better reflect the physics of the current setup a custom defined liquid density is also provided in the subroutine usr_prop_ros using the density model indicated in Table 5. This subroutine can then be accessed by invoking the appropriate keyword in the input file: `USR_ROS(1)=.TRUE.`. To satisfy MFIX error checks the density of the packing phase must also be specified, however, the precise value does not matter as it does not enter any calculations. For a non-reacting flow simulation a constant value for liquid density should be specified in the input file to avoid potential issues with undefined quantities in the evaluation of the model.

Depending on the phase, viscosity may be specified either as a constant value in the input file, or as a calculated value using either a default model or through a customized user routine in the file usr_properties.f. In MFIX, the default model for the gas phase viscosity is based on Sutherland's formula applied to air (Arnold, 1933; Sutherland, 1893). The default viscosity model for the liquid phase is established through a combination of keyword settings that ultimately result in a model founded for granular materials. Recall MFIX was originally designed for modeling gas-solids flow. To disable such a description requires specifying a constant value in the input file or through the customized user routine. A custom defined liquid viscosity is provided in the subroutine usr_prop_mus using the liquid viscosity model indicated in Table 5, below. This subroutine can then be accessed by invoking the appropriate keyword in the input file: `USR_MUS(1)=.TRUE.`. To satisfy MFIX error checks and/or avoid unwanted calculations the viscosity of the packing phase must also be specified, however, the precise value does not matter as it does not enter any calculations. For a non-reacting flow simulation a constant value for liquid viscosity should be specified in the input file to avoid potential issues with undefined quantities in the evaluation of the model.

5.2 HEAT AND MASS TRANSFER MODEL & PARAMETERS

The gas absorption with chemical reaction model introduced by Pandya (Pandya, 1983), discussed earlier, is used in this effort. This model accounts for mass-transfer resistance in both phases and chemical reaction in the liquid phase. To implement the CO_2–MEA chemistry as a reaction model into MFIX requires working within the construct of the existing CFD framework.

Specifically, details of the chemical reaction scheme are contained in the input file and in the subroutine usr_rates in the user file usr_rates.f. For further details on specifying reaction chemistry see the MFIX user guide f.

The gas phase is considered to be comprised of 3 species: Air, H_2O and CO_2. The liquid phase is comprised of 9 species: CO_2, R_1R_2NH, $R_1R_2NH_2^+$, $R_1R_2NCOO^-$, HCO_3^-, OH^-, CO_3^{2-}, H_3O^+, and H_2O. These species are specified in the input file, and are summarized in Table 4.

Table 4. Species Involved in the Chemistry for CO_2 Absorption into Aqueous MEA Solutions and their MFIX Alias

Species	Chemical formula	MFIX Species Alias	Mol. Wt. [g/mol]
Air (g)	Air	AIR	29.0000
Carbon dioxide (g)	$CO_2(g)$	gCO2	44.0095
Water vapor (g)	H_2O	gH2O	18.0152
Carbon dioxide (l)	$CO_2(l)$	lCO2	44.0095
Monoethanolamine (l)	R_1R_2NH	lRNH2	61.0828
Protonated MEA (l)	$R_1R_2NH_2^+$	RNH3p	62.0907
Bicarbonate (l)	HCO_3^-	HCO3m	61.0168
Hydroxide (l)	OH^-	OHm	17.0073
Carbonate (l)	CO_3^{--}	CO3m2	60.0089
Hydronium (l)	H_3O^+	H3Op	19.0231
Carbamate (l)	$R_1R_2NCOO^-$	RNHCO2m	104.0844
Water (l)	H_2O	lH2O	18.0152

In the CO_2–MEA system, CO_2 is first absorbed into the aqueous phase, followed by a set of homogenous liquid phase reactions. In the current implementation the CO_2 transfer from the gas to the liquid phase in the absorber is described using a single irreversible reaction in MFIX,

$$CO_2(g) \rightarrow CO_2(l)\ . \tag{54}$$

This reaction is specified in the input file. The rate at which the CO_2 transfer occurs is computed in usr_rates.f and given according to the flux expression for CO_2 (Equation 35) with the formula for interfacial pressure (Equation 37) using the contribution of the enhancement factor (see Equations 38-40).

Care must be taken when implementing a liquid phase reaction scheme so as not to incorporate the chemical reaction of CO_2 with MEA more than once. In particular if the rate of transfer of CO_2 from gas to liquid phase is described using an enhancement factor, then it would be redundant to consider an additional kinetic reaction of CO_2 with MEA in solution (Reaction 22). Such a description would make the overall model inconsistent as the effect of chemical reaction of CO_2 with MEA is already encompassed into the rate description through the enhancement factor. Instead, any liquid phase chemical reactions should be posed as equilibrium reactions (Reactions 24-28). However, implementing instantaneous equilibrium reactions within the traditional MFIX reaction framework poses certain challenges. Specifically, large reaction rates

chosen to facilitate fast equilibration can result in numerical instability when solving the species conservation equation[5].

In light of these issues, three different chemical reaction schemes have been implemented in the model. For low CO_2 loadings ($mol\ CO_2/mol\ R_1R_2NH < 0.5$), it has been suggested that the overall reaction between CO_2 and MEA in the liquid phase can be adequately represented using the single step irreversible process (Reaction 22) and equilibrium reactions do not need to be considered. For higher CO_2 loadings, it may be necessary to consider interaction of all species in the liquid bulk in order to obtain correct prediction of the loaded amine solution composition and absorption rates of CO_2. To do this requires introducing the equilibrium Reactions 24-28. Additionally, it may be necessary to reconsider the validity of the simplified kinetic rate expression (Equation 21), but this is left for a later effort. A total of six liquid phase reactions are specified in the MFIX input file (1 kinetic, 5 equilibrium). Each equilibrium reaction is specified as a separate forward and reverse reaction, meaning a total of 12 reaction rates (including for CO_2 absorption) need to be set in the subroutine usr_rates. The user can select from one of the three available schemes for setting these rates by changing the value of `ABSORPTION_CHEM_SCHEME` in the input file to one of the following:

5.2.1 ABSORPTION_CHEM_SCHEME = SINGLE_STEP

Chemical equilibrium in the liquid phase is ignored, and only the single step approximate kinetic reaction of CO_2 with MEA (Reaction 22) is considered. The rate for this reaction is given by the second order rate expression (Equation 23) and the kinetic expression of Hikata, (Equation 23) and is set in usr_rates.f. The enhancement factor for mass transfer is set to one, corresponding to pure physical mass transfer. In this case, only the concentration of liquid phase species $CO_2(l)$, R_1R_2NH, $\mathrm{R_1R_2NCOO^-}$, and $R_1R_2NH_2^+$ will evolve due to chemical reaction. As they do not participate in any reactions, the concentrations of HCO_3^-, OH^-, CO_3^{2-}, H_3O^+, and H_2O will remain fixed. Rates for all equilibrium reactions are set to zero in subroutine usr_rates of usr_rates.f.

5.2.2 ABSORPTION_CHEM_SCHEME = EQUILIBRIUM_SEGREGATED

In this scheme, forward and reverse rates for the five liquid equilibrium reactions 24-28 are defined in subroutine usr_rates of usr_rates.f. This is accomplished by choosing an forward rate constant, k_{fwd}, for each reaction, and using the definition of the equilibrium constant to set the reverse rate constant according to $k_{rev} = K/k_{fwd}$, where K is the equilibrium constant for the reaction (Equation 34) The kinetic conversion of CO_2 and MEA (Reaction 22) is not considered and the mass transfer enhancement factor is computed according to the Wellek (Wellek et al., 1978) model (Equation 38). This scheme is straight-forward and fits well within the existing MFIX framework. However, in practice, the rate of equilibration of the liquid phase species and stability of the species conservation equation solver are quite sensitive to the choice of k_{fwd} for each reaction. By default, all values of k_{fwd} are set to 1.0. However, the user can tune the value

[5] A stiff chemistry solver is available in MFIX, which might alleviate this problem, but currently only works for gas phase reactions.

of k_{fwd} for each reaction through the keyword C in input file. For more detail see Table 3, the input file and relevant subroutines. For the present set of equilibrium reactions, an equilibrium state was achieved following a finite period of time when the forward rate constants were set so that the reverse reaction rate constants become equal to a value of 108.

5.2.3 ABSORPTION CHEM SCHEME = EQUILIBRIUM COUPLED

In this scheme, a dedicated equilibrium chemistry solver is used to enforce chemical equilibrium of the nine liquid phase species at the beginning of each time step. This is accomplished by solving the coupled equilibrium constraints (Equations 29-33) for the equilibrium molar concentrations of each species. The liquid phase mass fractions are then updated directly before the species conservation equation is solved. The rates of the forward and reverse equilibrium reactions are set to zero in the subroutine usr_rates of usr_rates.f to null their contribution to the species equations. This approach effectively divorces the equilibrium reactions from the solution of the species transport equation, but has the advantage of being both fast and robust for a wide range of CO_2 loadings. The solver is called from subroutine usr1 in the file usr1.f and is provided as a module in the same file. While it is currently specific to the $CO_2 - MEA - H_2O$ chemistry, generalization is possible and it should be straightforward to modify the solver in order to study other amine based solvents. As in the EQUILIBRIUM_SEGREGATED scheme, Reaction 22 is not considered and the mass transfer enhancement factor is computed according to the Wellek (Wellek et al., 1978) model.

5.3 REACTION MODEL PARAMETERS

As noted earlier, calculations in the absorption-rate kinetics model also requires knowledge of the physical-chemical properties of the fluids (gas and liquid) involved in the process. This includes density, viscosity, solubility, diffusivity and surface tension. Varying physical properties are considered in the reaction model using published data from the literature as summarized in this table. These correlations incorporated in the usr_mod.f file as individual subroutines, which are then called in the relevant section within the overall code.

Table 5. Physical and Chemical Properties

Property	Reference
Liquid Viscosity, μ_l	Weiland (Weiland, Dingman, Cronin, & Browning, 1998)
Liquid Surface tension, σ_l	Vazquez (Vazquez, Alvarez, Navaza, Rendo, & Romero, 1997) see also Hiwale (Hiwale et al., 2012)
Liquid Density, ρ_l	Weiland (Weiland et al., 1998)
Diffusivity of CO_2 in MEA solution, $\mathcal{D}_{CO_2,l}$	Versteeg (Versteeg & van Swaaij, 1988)
Diffusivity of MEA in MEA solution, $\mathcal{D}_{MEA,l}$	Snijder (Snijder, te Riele, Versteeg, & van Swaaij, 1993)
Henry's constant for CO_2 in MEA, H	Versteeg (Versteeg & van Swaaij, 1988) see also Hiwale (Hiwale et al., 2012)

As indicated in Table 3 several user defined options are available to evaluate the fractional wetted area through the keyword `wetarea_type`. The fractional wetted area formulation outlined in Equation 42 corresponds to option `'ONDA_68'`. Other options include a model based on the work of Lappalainen et al. (Lappalainen et al., 2008) or a user specified constant value. If a constant value is wanted, then the keyword `wetareafrac0`should be defined according to the desired value. If the keyword, `wetarea_type` is undefined then the fractional wetted area is given a value of 1 (i.e., fully wet).

To evaluate the correlations for wetted area and gas and liquid side mass transfer coefficients (see Equations 42, 43 and 44), values for the specific area of packing (a_t) nominal size of the packing (D_p), and surface tension of the packing (σ_c) are needed. Their values will depend on the specific packing material. To specify these values new keywords were introduced into MFIX (see Table 3) as a_t =`sa_pack`, D_p =`dp_pack`, and σ_c =`omega_pack`. These should be set in the input file. Recall, the nominal size of the packing material is, by default, assigned to the diameter of 'solids' phase 2 (i.e., D_p =`d_p0(2)`). In these expressions, $\mathcal{D}_{g,s}$ is taken as the diffusivity of CO_2 in air, and is assigned a constant value $\left(\mathcal{D}_{g,s} = 0.16\frac{cm^2}{s}\right)$, and $\mathcal{D}_{l,s}$ is taken as the diffusivity of CO_2 in MEA solution $\left(\mathcal{D}_{l,s} = \mathcal{D}_{l,CO_2}\right)$. Finally it is worth noting that the wetted area of the packing (a_w) may also be set to a constant value through the input file using the keyword `wetarea_pack0`. However, if left undefined, then the model indicated by Equation 42 is used to evaluate this quantity.

5.4 SPECIES MASS TRANSFER PARAMETERS

As evident the problem of mass transfer in absorbers in complex due to the nature of mass transfer with chemical reaction. To fully close the chemical species mass balance equation (Equation 3) requires a value for the diffusion coefficient of the n^{th} chemical species in its respective phase ($\mathcal{D}_{g,n}$ and $\mathcal{D}_{l,n}$). By default MFIX effectively defines single diffusion coefficient for each phase, that is, $\mathcal{D}_{g,n} = D_g$ and $\mathcal{D}_{l,n} = D_l$. Diffusivity of each phase may be specified either as a constant value in the input file, or as a calculated value using either a default model or through a customized user routine found in the file usr_properties.f. In MFIX the default model for gas phase diffusivity is that of CO_2 in N_2 with the influence of gas temperature and pressure according to the Fuller relation (Fuller, Schettler, & Giddings, 1966). By default, MFIX assigns the liquid phase diffusivity to zero (i.e., no diffusion). To better reflect the physics of the current setup a custom defined liquid diffusivity is provided in the subroutine usr_prop_difs using the diffusivity model for CO_2 in MEA solution ($D_l = \mathcal{D}_{CO_2,l}$; see Table 5). This subroutine may be accessed by invoking the appropriate keyword in the input file: `USR_DIFS(1)=.TRUE.`.

5.5 HEAT TRANSFER PARAMETERS

To fully close the energy balance equation requires, among others, the specific enthalpies of each of the species present, which is calculated by combining the heat of formation with the integration of the specific heat of that species from the reference temperature. Thus, for evaluation, this information is needed for all species in each phase present. The database of Burcat and Ruscic (Burcat & Ruscic, 2005) is linked to MFIX and contains the necessary thermochemical data for those species that are listed. For the present case all the species making

up the gas phase (Air, H_2O and CO_2) are contained in the database. Liquid water is also available, however, the remaining 8 liquid phase species (CO_2, R_1R_2NH, $R_1R_2NH_2^+$, $R_1R_2NCOO^-$, HCO_3^-, OH^-, CO_3^{2-}, H_3O^+) are not listed in the database. Heat of formation data is available for 7 of the species (R_1R_2NH, $R_1R_2NH_2^+$, $R_1R_2NCOO^-$, HCO_3^-, OH^-, CO_3^{2-}, H_3O^+) and the heat capacity value is available for MEA species (Dugas, Alix, Lemaire, Broutin, & Rochelle, 2009; Linstrom & Mallard, Accessed 2016). As a result the specific heat of the 8 liquid phase species are specified equal to that of the MEA species until more appropriate information can be obtained. This information is specified in the input file.

Additional properties that must be defined include the specific heat and thermal conductivities of each phase (C_{pi} and λ_i). By default, the specific heat of each phase is calculated based on mass average of the specific heat of each chemical species present in that phase. Like diffusivity, conductivity of each phase may be specified either as a constant value in the input file, or as a calculated value using either a default model or through a customized user routine in the file usr_properties.f. In MFIX the default model for gas phase conductivity is set to that of air at 300 K with a temperature dependent term (Bird, Stewart, & Lightfoot, 1960). By default MFIX calculates the liquid and solids phase conductivity based on a model of a solids phase that is comprised of discrete ash particles. See (Syamlal et al., 1993) for details. To better reflect the physics of the current setup a custom defined liquid phase conductivity is specified in the subroutine usr_prop_ks using the correlation for aqueous MEA by Cheng (Cheng, Meisen, & Chakma, 1996). This subroutine can then be accessed by invoking the appropriate keyword in the input file: `USR_KS(1)=.TRUE.`.

5.5.1 Interphase Heat Transfer by Convection

The general form of the interphase heat transfer term as a function of the temperature difference indicated by Equations 45 and 46 is already incorporated into MFIX. In MFIX, the corresponding heat transfer coefficients are based on either the default model or through a customized user routine in the file usr_properties.f. In MFIX, the default heat transfer coefficient model is based on a Nusselt correlation for particles in packed or fluidized bed (Gunn, 1978) with a correction for interphase mass transfer (Bird et al., 1960). See (Syamlal et al., 1993) for details. To better reflect the physics of the current setup custom defined heat transfer coefficients are specified based on Equations 48 and 52 in the subroutine usr_prop_gama. This routine may be accessed by invoking the appropriate keyword in the input file: `USR_GAMA(1)=.TRUE.` and `USR_GAMA(2)=.TRUE.`

5.5.2 Interphase Heat Transfer by Interphase Mass Transfer

Closure for interphase enthalpy transfer accompanying interphase mass transfer is implicitly calculated in the code provided the appropriate information for the specific enthalpies of the relevant species involved is given. Unfortunately not all of this information is available. As a result, in this case the calculation is superseded by explicitly defining a 'heat of reaction' for the indicated reaction and partitioning this energy between the associated phases. This information is specified in the input file (see MFIX user guide). Heat of absorption data has been reported for CO_2 into MEA (Gabrielsen, Michelsen, Stenby, & Kontogeorgis, 2005). This information is used to specify a heat of reaction for this reaction which is then partitioned fully to the liquid phase. The heat of reaction for each of the liquid phase reactions is explicitly set to zero until more appropriate information may be obtained.

6. MFIX SIMULATION STUDY

6.1 SYSTEM DESCRIPTION

In this tutorial counter current gas-liquid flow through a packed column is simulated using MFIX. A schematic of the simulation setup is present in Figure 1a. The column is 180 cm in height and 15cm in inner diameter. A two dimensional approximation of the column is made in the Cartesian coordinate system so that only the center-plane is effectively simulated. The mesh is comprised of 32x360x1 elements. Three continuous phases are employed (`MMAX=2`). In the present work the gas phase is treated as phase 0. Two additional continuous 'solids' phases are employed to model the liquid and packing material. The liquid phase is taken as solids phase 1 (`M=1`) while the packing material is taken as solids phase 2 (`M=2`).

The gas phase is defined as a mixture of air, CO_2 and H_2O vapor. The liquid phase is defined as a mixture of the 9 species in Table 4. The properties of the liquid phase may also be varied according to one's needs and by using the user defined property functions summarized earlier and in Table 5. The bottom and top 20cm of the domain are inlet and outlet plenums. In between, the absorption column is represented as a stationary solid phase, with constant uniform solid fraction, $\epsilon_s = 0.06$. More complex distribution of solids volume fraction may be assigned at the beginning of the simulation, which remains invariant throughout the simulation. Accordingly, the domain effectively consists of a porous media defined by solids phase 2. The packing material consists of metal Bialecki rings having a specific packing area ($a_t =$ `sa_pack`) of 2.38 cm^2/cm^3 and nominal size ($D_p =$`dp_pack`) of 2.55cm. Therefore, an equivalent particle diameter ($d_p =$`d_p0(2)`) can be calculated as 0.1512 cm. This physical configuration is based on the experimental work of (Billet, 1995). A critical surface tension of the packing ($\sigma_c =$ `omega_pack`) is defined as 61 dyne/cm (Pacheco, 1998) .

In this demonstration case the default values of 180 and 1.8 for the viscous and inertial constants, respectively, in the three interaction models are not used. Instead they are independently modified using through the keyword `C` in the input file. In this case the viscous and the inertial coefficients in the gas-liquid interaction term (Equation 15) are defined as 0.18 and 0.225, respectively. Similarly, the viscous and inertial coefficients of the gas-solids (Equation 16) and liquid-solids (Equation 17) interaction terms are as follows: 182, 2.46, 0.18 and 1.093, respectively. These were found from an optimization analysis based on the experimental data not discussed herein. For more detail see the input file and relevant subroutines.

Initially, the liquid phase is not present in the domain, and the gas phase is 100% air. The liquid phase is injected into the domain via a point source located just above the packing material as shown. The liquid mass flow rate, $\dot{m}_l = 16.7\ g/s$, is defined in the input file and while not required, the liquid velocity is also specified as $-0.62 m/s$ in the *y* direction. This corresponds to a superficial liquid velocity, $u_l = 40\ m/h$. The top of the column is defined using a pressure outlet boundary condition with the outlet pressure set to 1013250 barye gauge. At the bottom of the domain, the gas and liquid may freely exit or enter through an inlet boundary condition at elevated pressure, P_{in}. The inlet pressure is set between set 1013810 barye and 1049090 bayre, so that the pressure drop is between 40 and 2560 Pa/m, similar to the range considered experimentally (Billet, 1995). Accordingly, the pressure drop is specified, while the inlet gas

flow rate becomes a result of the simulation setup. The composition of the gas and liquid at their inlet boundaries depend on the simulation as discussed below.

The setup is summarized here. For greater detail, including settings used for model options described in Table 3, see the input file.

Computational/Physical model

3D, transient, slightly compressible
Multi-phase: gas (M=0), liquid (M=1), structure via porous media (M=2)
Gravity: $-981\frac{cm}{s^2}$ in *y* direction
Momentum equations: solved for M=0 and M=1 (Ishii form) not solved for M=2
Thermal energy equations are solved
Turbulence equations are not solved (Laminar)
Uniform Mesh
Superbee scheme

Geometry	
Coordinate system	Cartesian
Domain length, L (x)	15.0 (cm)
Domain height, H (y)	180.0 (cm)
Domain width, W (z)	1.0 (cm)
Material 0 (M=0; gas-phase)	
Fluid density, ρ_g	1.2 (g·cm^{-3})
Fluid viscosity, μ_g	1.0 (Poise)
Material 1 (M=1; liquid-phase)	
Diameter†	0.2 (cm)
Density, ρ_l	1.0 (g·cm^{-3})
Fluid viscosity, μ_l	0.01 (Poise)
Material 2 (M=2; packing)	
Diameter, d_p	0.1512 (cm)
Density†	5.0 (g·cm^{-3})
Fluid viscosity†	0.01 (Poise)
Initial Conditions	
Pressure *(gauge)*, P_g	
Fluid x-velocity, u_g	.0 (cm·s^{-1})
Fluid y-velocity, v_g	.0 (cm·s^{-1})
Fluid z-velocity, w_g	.0 (cm·s^{-1})
Fluid x-velocity, u_l	.0 (cm·s^{-1})
Fluid y-velocity, v_l	.0 (cm·s^{-1})
Fluid z-velocity, w_l	.0 (cm·s^{-1})
Boundary Conditions‡	
Wall boundaries	No-slip wall
Top boundary	Pressure outflow
Bottom boundary	Pressure inflow
Liquid inlet	Point source

† Material properties selected to satisfy MFIX error checks but not used in calculation.
‡ Flag specified to minimize unnecessary calculations in MFIX and ensure porous media treatment

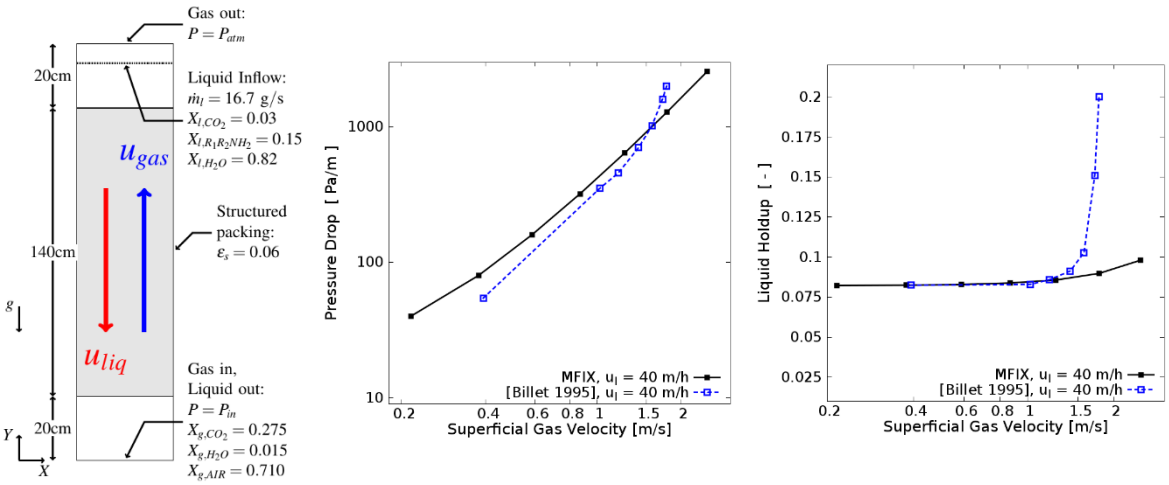

(a) Configuration (b) Gas-pressure drop (c) Liquid holdup

Figure 1. MFIX simulation study of CO_2 absorption in a counter flow gas-liquid absorption column. (a) Simulation configuration and boundary conditions with the composition of entering gas/liquid set to either pure air/water or the composition indicated depending on the simulation. (b)-(c) Pressure drop and liquid holdup vs superficial gas velocity, compared to the air/water experimental data of Billet (1995).

As a preliminary validation of the three-phase hydrodynamics in the model, the simulated pressure drop and liquid holdup are compared to the experimental data of Billet (1995) in Fig. 1b and Fig 1c. To be consistent with the experiments, the gas and liquid phase properties were fixed to those of air and water. The variation in pressure drop results in average superficial gas velocities in the range $0.22m/s \leq u_g \leq 2.47m/s$ (corresponding to gas mass flow rates between 0.39 g/s and 4.45 g/s). Reasonable agreement with the experiments is obtained over most of the range of superficial gas velocities, although the sharp rise in liquid holdup at high gas velocity is not predicted by the present model. It is likely that these results could be improved in the future by considering a fully 3D domain with wall effects, and also through improved correlations for wetted area and interphase momentum exchange coefficients as they become available.

Next we consider absorption of CO_2 into an aqueous MEA solution in the same domain. The liquid phase at the inlet is characterized as a 15% wt aqueous MEA solution with CO_2 loading of 0.277 (mol CO_2/mol MEA) and a temperature of 300K. The inlet gas composition is 27% wt CO_2 and 1.5% wt H_2O vapor at a slightly elevated temperature of 313K. The reacting flow was activated using the `EQUILIBRIUM_COUPLED` scheme described previously, and the evolution of the gas and liquid species in the column was simulated for an inlet pressure of $P_{in} = 1049090\ bayre$ ($\Delta P = 2560\ Pa/m$). At this gas flow rate, the liquid holdup is increased to approximately 10% and the gas/liquid flow is unsteady, resulting in a complex distribution of the reacting liquid species, as shown in Figure 2a. For this CO_2 loading, the equilibrium chemistry solver predicts there are five species (in addition to water), with significant mass fractions along the column: CO_2, HCO_3, R_1R_2NH, $R_1R_2NCOO^-$, and $R_1R_2NH_2^+$. The mass fraction of all other species (excluding H_2O) is negligible.

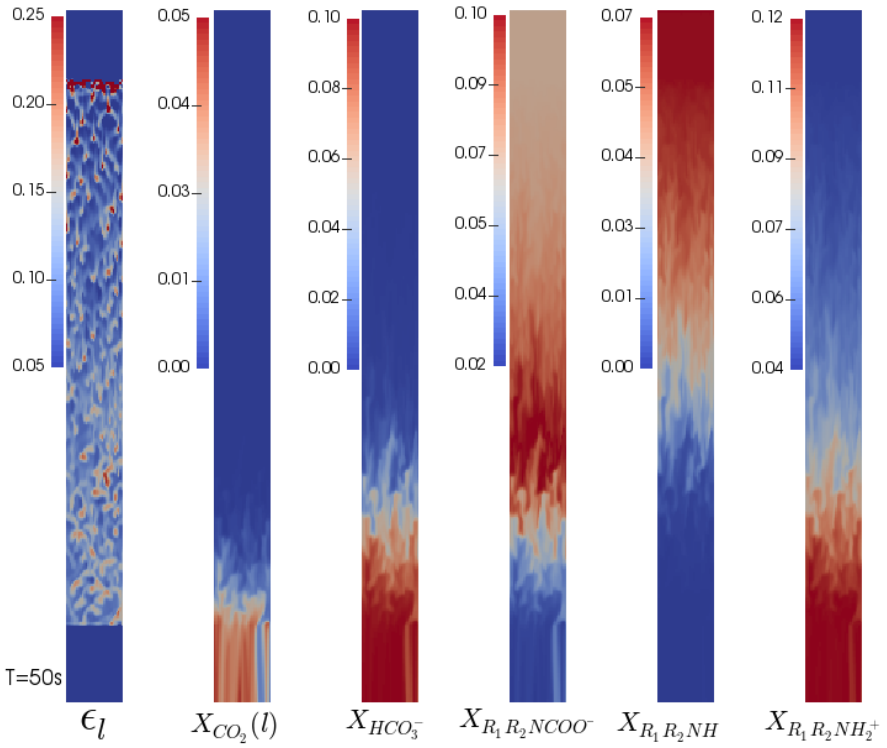

(a) Instantaneous contours of liquid fraction (ϵ_l) and liquid species mass fraction (X_i)

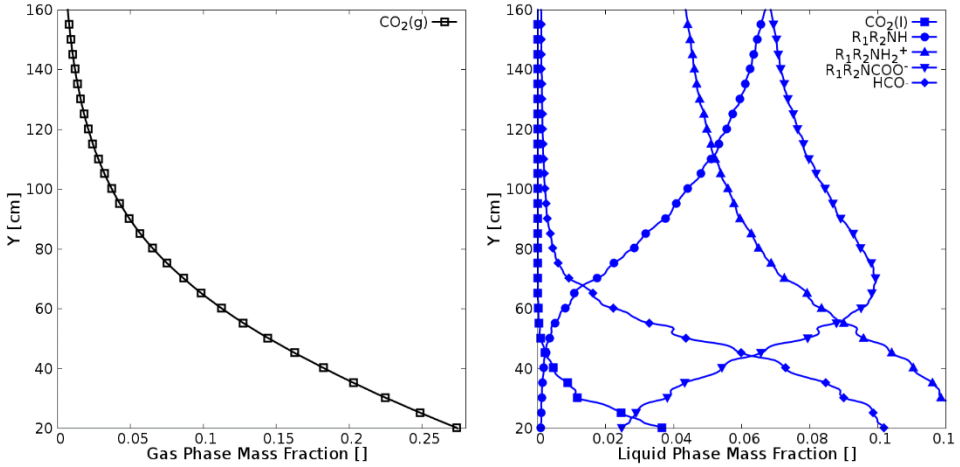

(b) Gas-phase CO_2 mass fraction (c) Liquid-phase mass fractions

Figure 2. Distribution of gas and liquid phase species in the column under absorber conditions. (a) Contours of liquid fraction and mass fraction of significant liquid phase species at one instant in time. (b) Steady state profile of gas phase CO_2 mass fraction. (c) Steady state profiles of the significant liquid phase species.

The absorption process appears to reach an equilibrium state (no temporal change in CO_2 mass fraction) after about t=20s. At this point, nearly all of the CO_2 is absorbed into the liquid by the time it reaches the top of the column as shown in Figure 2b. In the liquid phase, the free $R_1R_2NH_2$ is consumed near the bottom of the column, resulting in a significant rise in the mass fraction of $R_1R_2NH_2^+$ and HCO_3 close to the gas inlet / liquid outlet (Figure 2c).

7. FINAL REMARKS

Flow distribution plays an important role in column efficiency and poor wetting, channeling and bypassing are potential issues that device-scale CFD may be able to capture that a 1D process model cannot. However, very little work has been done in this regard. The goal here was to develop a device scale CFD model (with and without reactions) in MFIX which can then be used to examine how these inhomogeneities may arise and their effect on reactor performance.

8. REFERENCES

Aboudheir, A., Tontiwachwuthikul, P., Chakma, A., & Idem, R. (2003). Kinetics of the reactive absorption of carbon dioxide in high CO2-loaded, concentrated aqueous monoethanolamine solutions. *Chemical Engineering Science, 58*(23-24), 5195-5210. doi: 10.1016/j.ces.2003.08.014

Arnold, J. H. (1933). Vapor viscosities and the sutherland equation. *Journal of Chemical Physics, 1*, 170-176.

Attou, A., Boyer, C., & Ferschneider, G. (1999). Modelling of the hydrodynamics of the cocurrent gas-liquid trickle flow through a trickle-bed reactor. *Chemical Engineering Science, 54*(6), 785-802. doi: Doi 10.1016/S0009-2509(98)00285-1

Attou, A., & Ferschneider, G. (1999). A two-fluid mdoel for flow regime transition in gas-liquid trickle-bed reactors. *Chemical Engineering Science, 54*, 5031-5037.

Billet, R. (1995). *Packed Towers in Processing and Environmental Technology* (J. Fullarton, Trans.). New York, NY: VCH.

Bird, B. R., Stewart, W. E., & Lightfoot, E. N. (1960). *Transport Phenomena*. New York: John Wiley & Sons.

Burcat, A., & Ruscic, B. (2005). Third millennium ideal gas and condensed phase thermochemical database for combustion with updates for active thermochemical tables. ANL_05/20 and TAE 960 Technion-IIT, Aerospace Engineering, and Argonne National Laboratory, Chemistry Division.

Caplow, M. (1968). Kinetics of Carbamate Formation and Breakdown. *Journal of the American Chemical Society, 90*(24), 6795-&. doi: Doi 10.1021/Ja01026a041

Cheng, S., Meisen, A., & Chakma, A. (1996). Predict amine solution properties accurately. *Hydrocarbon Processing, 75*(2), 81-84.

Crooks, J. E., & Donnellan, J. P. (1989). Kinetics and Mechanism of the Reaction between Carbon-Dioxide and Amines in Aqueous-Solution. *Journal of the Chemical Society-Perkin Transactions 2*(4), 331-333. doi: Doi 10.1039/P29890000331

Danckwerts, P. V. (1979). Reaction of Co2 with Ethanolamines. *Chemical Engineering Science, 34*(4), 443-446. doi: Doi 10.1016/0009-2509(79)85087-3

Dudukovic, M. P., Larachi, F., & Mills, P. L. (2002). Multiphase catalytic reactors: a perspective on current knowledge and future trends. *Catalysis Reviews: Science and Engineering, 44*(1), 123-246. doi: Doi 10.1081/Cr-120001460

Dugas, R., Alix, P., Lemaire, E., Broutin, P., & Rochelle, G. (2009). Absorber model for CO_2 capture by monoethanolamine - application to CASTOR pilot results. *Energy Procedia, 1*, 103-107. doi: http://dx.doi.org/10.1016/j.egypro.2009.01.016

Edwards, T. J., Maurer, G., Newman, J., & Prausnitz, J. M. (1978). Vapor-liquid equilibria in multicomponent aqueous solutions of volatile weak electrolytes. *AIChE Journal, 24*(6), 966-976.

Fourati, M., Roig, V., & Raynal, L. (2013). Liquid dispersion in packed columns: Experiments and numerical modeling. *Chemical Engineering Science, 100*, 266-278. doi: 10.1016/j.ces.2013.02.041

Fuller, E. N., Schettler, P. D., & Giddings, J. C. (1966). A new method for prediction of binary gas-phase diffusion coefficients. *Industrial and Engineering Chemistry, 58*(5), 18-27.

Gabrielsen, J., Michelsen, M. L., Stenby, E. H., & Kontogeorgis, G. M. (2005). A Model for Estimating CO2 Solubility in Aqueous Alkanolamines. *Industrial & Engineering Chemistry Research, 44*(9), 3348-3354. doi: 10.1021/ie048857i

Grosser, K., Carbonell, R. G., & Sundaresan, S. (1985). Onset of Pulsing in Two-Phase Cocurrent Downflow through a Packed Bed. *AIChE Journal, 34*(11), 1850-1860.

Gunjal, P. R., Kashid, M. N., Ranade, V. V., & Chaudhari, R. V. (2005). Hydrodynamics of trickle-bed reactors: Experiments and CFD modeling. *Industrial & Engineering Chemistry Research, 44*(16), 6278-6294. doi: 10.1021/ie0491037

Gunjal, P. R., & Ranade, V. V. (2007). Modeling of laboratory and commercial scale hydro-processing reactors using CFD. *Chemical Engineering Science, 62*(18-20), 5512-5526.

Gunn, D. J. (1978). Transfer of Heat or Mass to Particles in Fixed and Fluidized-Beds. *International Journal of Heat and Mass Transfer, 21*(4), 467-476. doi: Doi 10.1016/0017-9310(78)90080-7

Hikita, H., Asai, S., Ishikawa, H., & Honda, M. (1977). The kinetics of reactions of carbon dioxide with monoethanolamine, diethanolamine and triethanolamine by a rapid mixing method. *The Chemical Engineering Journal, 13*, 7-12.

Hiwale, R., Hwang, S., & Smith, R. (2012). Model building methodology for multiphase reaction systems – modeling of CO_2 absorption in monoethanolamine for laminar jet absorbers and packing beds. *Industrial & Engineering Chemistry Research, 51*(11), 4328-4346. doi: DOI 10.1021/ie201869w

Holub, R. A., Dudukovic, M. P., & Ramachandran, P. A. (1992). A Phenomenological Model for Pressure-Drop, Liquid Holdup, and Flow Regime Transition in Gas-Liquid Trickle Flow. *Chemical Engineering Science, 47*(9-11), 2343-2348. doi: Doi 10.1016/0009-2509(92)87058-X

Iliuta, I., & Larachi, F. (1999). The generalized slit model: pressure gradient, liquid holdup & wetting efficiency in gas-liquid trickle flow. *Chemical Engineering Science, 54*, 5039-5045.

Jiang, Y., Khadilkar, M. R., Al-Dahhan, M. H., & Dudukovic, M. P. (2002). CFD of multiphase flow in packed-bed reactors: I. k-fluid modeling issues. *AIChE Journal, 48*(4), 701-715. doi: DOI 10.1002/aic.690480406

Kent, R. L., & Eisenberg, B. (1976). Better data for amine treating. *Hydrocarbon Process, 55*, 87-90.

Kuzeljevic, Z. V., & Dudukovic, M. P. (2012). Computational Modeling of Trickle Bed Reactors. *Industrial & Engineering Chemistry Research, 51*(4), 1663-1671. doi: 10.1021/ie2007449

Lappalainen, K., Alopaeus, V., Manninen, M., & Aittamaa, J. (2008). Improved hydrodynamic model for wetting efficiency, pressure dorp, and liquid holdup in trickle-bed reactors. *Industrial & Engineering Chemistry Research, 47*, 8436-8444.

Lappalainen, K., Gorshkova, E., Manninen, M., & Alopaeus, V. (2011). Characteristics of liquid and tracer dispersion in trickle-bed reactors: Effect on CFD modeling and experimental analyses. *Computers & Chemical Engineering, 35*(1), 41-49. doi: 10.1016/j.compchemeng.2010.06.006

Lappalainen, K., Manninen, M., & Alopaeus, V. (2009). CFD modeling of radial dspreading of flow in trickle-bed reactors due to mechanical and capillary dispersion. *Chemical Engineering Science, 64*, 207-218.

Lappalainen, K., Manninen, M., Alopaeus, V., Aittamaa, J., & Dodds, J. (2009). An Analytical Model for Capillary Pressure-Saturation Relation for Gas-Liquid System in a Packed-Bed of Spherical Particles. *Transport in Porous Media, 77*(1), 17-40. doi: 10.1007/s11242-008-9259-z

Levenspiel, O. (1999). *Chemical Reaction Engineering* (3rd ed.). New York, USA: John Wiley & Sons, Inc.

Linstrom, P. J., & Mallard, W. G. (Eds.). (Accessed 2016). *NIST Chemistry WebBook*. National Institute of Standards and Technology, Gaithersburg MD, 20899: http://webbook.nist.gov.

Mackowiak, J. (2010). *Fluid Dynamics of Packed Columns* (C. Hall, Trans.): Springer-Verlag Berlin Heidelberg.

Musser, J., Syamlal, M., Shahnam, M., & Huckaby, D. (2015). Constitutive equation for heat transfer caused by mass transfer. *Chemical Engineering Science, 123*(17), 436-443.

Onda, K., Takeuchi, H., & Okumoto, Y. (1968). Mass transfer coefficients between gas and liquid phases in packed columns. *Journal of Chemical Engineering of Japan, 1*(1), 56-62.

Pacheco, M. A. (1998). *Mass Transfer, Kinetics and Rate-based Modeling of Reactive Absorption.* (Doctor of Philosophy Ph.D.), University of Texas, Austin, Texas.

Pandya, J. D. (1983). Adiabatic Gas-Absorption and Stripping with Chemical-Reaction in Packed Towers. *Chemical Engineering Communications, 19*(4-6), 343-361. doi: Doi 10.1080/00986448308956351

Ranz, W. E., & Marshall, W. R. J. (1952). Evaporation from Drops: Part II. *Chemical Engineering Progress, 48*(4), 173-180.

Raynal, L., Ben Rayana, F., & Royon-Lebeaud, A. (2009). Use of CFD for CO2 absorbers optimum design : from local scale to large industrial scale. *Energy Procedia, 1*(1), 917-924.

Raynal, L., Boyer, C., & Ballaguet, J. P. (2004). Liquid holdup and pressure drop determination in structured packing with CFD simulations. *Canadian Journal of Chemical Engineering, 82*(5), 9.

Razi, N., Bolland, O., & Svendsen, H. (2012). Review of design correlations for CO2 absorption into MEA using structured packings. *International Journal of Greenhouse Gas Control, 9*, 193-219. doi: 10.1016/j.ijggc.2012.03.003

Saez, A. E., & Carbonell, R. G. (1985). Hydrodynamic Parameters for Gas-Liquid Cocurrent Flow in Packed-Beds. *AIChE Journal, 31*(1), 52-62. doi: DOI 10.1002/aic.690310105

Snijder, E. D., te Riele, M. J. M., Versteeg, G. F., & van Swaaij, W. P. M. (1993). Diffusion coefficients of several aqueous alkanolamine solutions. *Journal of Chemical and Engineering Data, 38*(3), 475-480. doi: Doi 10.1021/Je00011a037

Solomenko, Z., Haroun, Y., Fourati, M., Larachi, F., Boyer, C., & Augier, F. (2015). Liquid spreading in trickle-bed reactors: Experiments and numerical simulations using Eulerian-Eulerian two-fluid approach. *Chemical Engineering Science, 126*, 698-710. doi: 10.1016/j.ces.2015.01.013

Sutherland, W. (1893). The viscosity of gases and molecular force. *Philosophical Magazine Series 5, 36*(223), 507-531. doi: 10.1080/14786449308620508

Syamlal, M., Rogers, W., & O'Brien, T. J. (1993). *MFIX Documentation Theory Guide*. (DOE/METC-94/1004 (DE94000087)). Morgantown, West Virginia.

Vazquez, G., Alvarez, E., Navaza, J. M., Rendo, R., & Romero, E. (1997). Surface tension of binary mixtures of water plus monoethanolamine and water plus 2-amino-2-methyl-1-propanol and tertiary mixtures of these amines with water from 25 degrees C to 50 degrees C. *Journal of Chemical and Engineering Data, 42*(1), 57-59. doi: Doi 10.1021/Je960238w

Versteeg, G. F., van Dijck, L. A. J., & van Swaaij, W. P. M. (1996). On the kinetics between CO2 and alkanolamines both in aqueous and non-aqueous solutions. An overview. *Chemical Engineering Communications, 144*(1), 113-158. doi: Doi 10.1080/00986449608936450

Versteeg, G. F., & van Swaaij, W. P. M. (1988). Solubility and Diffusivity of Acid Gases (CO2, N2O) in Aqueous Alkanoalmine Solutions. *Journal of Chemical and Engineering Data, 33*, 29-34.

Wang, G. Q., Yuan, X. G., & Yu, K. T. (2005). Review of mass-transfer correlations for packed columns. *Industrial & Engineering Chemistry Research, 44*(23), 8715-8729. doi: 10.1021/ie050017w

Weiland, R. H., Dingman, J. C., Cronin, D. B., & Browning, G. J. (1998). Density and viscosity of some partially carbonated aqueous alkanolamine solutions and their blends. *Journal of Chemical and Engineering Data, 43*(3), 378-382. doi: Doi 10.1021/Je9702044

Wellek, R. M., Brunson, R. J., & Law, F. H. (1978). Enhancement factors for gas-absorption with second-order irreversible chemical reaction. *The Canadian Journal of Chemical Engineering, 56*, 181-186.

Sean Plasynski
Executive Director
Technology Development & Integration Center
National Energy Technology Laboratory
U.S. Department of Energy

Cynthia Powell
Executive Director
Research and Innovation Center
National Energy Technology Laboratory
U.S. Department of Energy

Lynn Brickett
Carbon Capture Technology Manager
Science and Technology Strategic Plans & Programs
National Energy Technology Laboratory
U.S. Department of Energy

David Miller
Senior Fellow
Science and Technology Strategic Plans & Programs
National Energy Technology Laboratory
U.S. Department of Energy

Isaac Aurelio
Carbon Capture Technical Monitor
Technology Development & Integration Center
National Energy Technology Laboratory
U.S. Department of Energy

Syamlal Madhava
Senior Fellow
Science and Technology Strategic Plans & Programs
National Energy Technology Laboratory
U.S. Department of Energy